Motion of three point vortices in a periodic parallelogram

By MARK A. STREMLER AND HASSAN AREF

Department of Theoretical and Applied Mechanics,
University of Illinois at Urbana-Champaign, Urbana, IL 61801-2983, USA

The motion of three interacting point vortices with zero net circulation in a periodic parallelogram defines an integrable dynamical system. A method for solving this system is presented. The relative motion of two of the vortices can be 'mapped' onto a problem of advection of a passive particle in 'phase space' by a certain set of stationary point vortices, which also has zero net circulation. The advection problem in phase space can be written in Hamiltonian form, and particle trajectories are given by level curves of the Hamiltonian. The motion of individual vortices in the original three-vortex problem then requires one additional quadrature. A complicated structure of the solution space emerges with a large number of qualitatively different regimes of motion. Bifurcations of the streamline pattern in phase space, which occur as the impulse of the original vortex system is changed, are traced. Representative cases are analysed in detail, and a general procedure is indicated for all cases. Although the problem is integrable, the trajectories of the vortices can be surprisingly complicated. The results are compared qualitatively to vortex paths found in large-scale numerical simulations of two-dimensional turbulence.

1. Introduction

In most numerical simulations of homogeneous, isotropic, two-dimensional turbulence the flow field is represented in a domain, usually taken as a square, that is periodically continued in both directions to provide a complete tiling of the plane. It is argued that the use of periodic boundary conditions in this way provides the best representation of a sample of the turbulence free from the effects of confining boundaries. As the turbulence evolves, one observes that strong, spatially localized vortices emerge, and at intermediate to late stages of such simulations a basic feature of the dynamics is the interaction of these strong vortices. At very late stages the presence of periodic boundaries becomes noticeable, and the flow relaxes to one with a small number of large vortices – typically two, one of each sign – which then decay by viscous effects.

During the period where one has several strong, well-defined, isolated vortices it is natural to track their trajectories. This has been done by several investigators (see for example McWilliams 1990). One is led to consider a model in which an assembly of N point vortices evolves within a finite, periodic domain. It is convenient to think of the flow plane as the complex z-plane, where $z = x + \mathrm{i}y$ represents a concatenation of the x- and y-coordinates. The periodic domain will have a shape characterized by two complex numbers, represented here as $2\omega_1$ and $2\omega_2$, which are the periods of the domain. The only constraint on these periods is that their ratio not be real, although typically ω_1 and ω_2 are chosen such that $\mathrm{Im}\,\omega_2/\omega_1 > 0$. Any two such numbers

define a tessellation of the plane into a lattice of identical 'period-parallelograms'; that period-parallelogram with vertices 0, $2\omega_1$, $2\omega_1 + 2\omega_2$, $2\omega_2$ is the 'fundamental period-parallelogram', which we will refer to simply as the fundamental parallelogram. A system of point vortices is placed in the fundamental parallelogram and periodically continued to all other parallelograms. Each 'base' vortex, thus, represents an infinite lattice (with generators $2\omega_1$ and $2\omega_2$) of identical vortices. With the base vortices at $z_\alpha = x_\alpha + iy_\alpha$, $\alpha = 1, \ldots, N$, vortex α has periodic images at $z_\alpha + 2m\omega_1 + 2n\omega_2$, where (m, n) is any pair of integers different from $(0, 0)$. Vortex α and its periodic images all have strength Γ_α.

Such vortex lattice problems date back to Tkachenko (1966), who derives equations of motion for a vortex lattice in terms of the Weierstrass ζ-function and applies these equations to the problem of a lattice of identical vortices that rotates rigidly. This work has been extended by O'Neil (1989) to the problem of N point vortices of various strengths arranged on N lattices that are allowed to rotate or translate as a whole. Benzi & Legras (1987) consider the related problem of N point vortices in a square domain with doubly periodic boundary conditions, deriving equations of motion in terms of infinite double sums over exponential and trigonometric functions. Campbell, Doria & Kadtke (1989), considering the same problem, derive equations of motion in terms of one infinite sum and one infinite product, both involving exponential and trigonometric functions. Most recently, Weiss & McWilliams (1991) derive equations of motion in a square domain in terms of an infinite sum over trigonometric and hyperbolic functions.

Similarly to the work of Benzi & Legras (1987), Campbell *et al.* (1989) and Weiss & McWilliams (1991), we impose periodicity of the flow field at the boundaries of the period-parallelograms. The periodicity of the flow field requires that the circulation integral around the boundary of any parallelogram must vanish. Thus, the circulations of the base vortices must sum to zero, which cannot, of course, be satisfied for $N = 1$. As we shall see below, this constraint implies that the system is integrable for $N = 2$ and 3. The solution for $N = 2$ is a uniform translation of all vortices with no relative motion. In this paper we show how to carry out the solution for $N = 3$, which is considerably richer than its counterpart on the infinite plane (Aref 1989; Rott 1989), and we display properties of the motion. Our methodology is an extension of a procedure recently used to solve the problem of three vortices with zero total circulation in a periodic strip (Aref & Stremler 1996; henceforth abbreviated AS). Note that in the strip case it is necessary to enforce the condition that the sum of the strengths is zero – this condition is equivalent to imposing periodicity of the flow for the periodic-parallelogram case. The results of AS can be obtained from the results presented here by setting Im $\omega_1 = 0$ and taking the limit Im $\omega_2 \to \infty$.

The three-vortex problem is of fundamental significance since it is the smallest one for which the separations between vortices change in time. These separations represent the 'scales of motion' in this problem, and a key dynamical feature of two-dimensional turbulence is the transfer of energy (and other quantities) between different scales. Elucidating a basic mechanism responsible for such transfer by solving the problem of three interacting vortices in a periodic domain may thus lead to a better understanding of two-dimensional turbulence dynamics, although the detailed execution of such a program is still at a very preliminary stage.

Our main objective in this paper is to solve the equations of vortex motion for the case $N = 3$ (and $\Gamma_1 + \Gamma_2 + \Gamma_3 = 0$) in a doubly periodic domain. As already mentioned, the equations of motion for the vortices in such a domain can be stated in various forms. In §2 we outline a derivation of the equations in terms of the

Weierstrass ζ-function. As in the periodic strip problem (cf. AS), the dynamics of the quantity $z_1 - z_2$ can be 'mapped' to an advection problem with stationary vortices. When the ratios between vortex strengths are rational, this advection problem takes place in a period-parallelogram with sides that are a multiple of the original. All relative motions of the vortices (except 'separatrix motions' connecting steady states) are then periodic. Derivation of the necessary formulae is presented in §3. Although always integrable, the advection problem becomes very complicated for all but the simplest rational ratios of vortex strengths. Thus, in §4 we consider the simplest case $\Gamma_1 : \Gamma_2 : \Gamma_3 = 1 : 1 : (-2)$. We also study the effects of varying the shape of the parallelogram in this case. For $\Gamma_1 : \Gamma_2 : \Gamma_3 = 2 : 1 : (-3)$ the dynamical problem is already quite rich; we discuss this case in detail for a square domain in §5. The reader may wish to glance at figure 12 to appreciate why venturing much beyond this case is, for all practical purposes, out of the question – this figure shows the separatrix streamlines of the advection problem corresponding to $\Gamma_1 : \Gamma_2 : \Gamma_3 = 7 : 3 : (-10)$. Higher rationals have not been attempted as the number of regimes of motion becomes unmanageably large, although the method that we provide gives a recipe for obtaining the solution in every case. When the ratios of vortex strengths are irrational, the advection problem does not 'fit' into a period-parallelogram, and the relative motion of the three interacting vortices can be non-periodic. These complications are discussed in §6. Finally, in §7 we make some remarks on the apparent correspondence of the complexity seen in this integrable problem and the vortex trajectories observed in large-scale simulations of two-dimensional turbulence.

2. Equations of motion

From a mathematical viewpoint, the conjugate velocity in the field of N point vortices with zero net circulation in a periodic parallelogram is given by a doubly periodic (complex-valued) function with N simple poles at z_β, $\beta = 1, \ldots, N$, with residues $\Gamma_\beta / 2\pi i$, respectively, and with the sum of the residues being zero. Such a function is an elliptic function. The sum of Weierstrass ζ-functions $(1/2\pi i) \sum_{\beta=1}^{N} \Gamma_\beta \zeta(z - z_\beta)$ is also an elliptic function having N simple poles at z_β, $\beta = 1, \ldots, N$, with residues $\Gamma_\beta / 2\pi i$, respectively. The Weierstrass ζ-function is defined by (Whittaker & Watson 1927, §20.4)

$$\zeta(z; \omega_1, \omega_2) = \frac{1}{z} + {\sum_{(m,n)}}' \left[\frac{1}{z - \Omega_{mn}} + \frac{1}{\Omega_{mn}} + \frac{z}{\Omega_{mn}^2} \right], \tag{2.1}$$

with $\Omega_{mn} = 2m\omega_1 + 2n\omega_2$ for integers m, n, and with the prime indicating that the sum is over all pairs of integers $(m, n) \neq (0, 0)$. By Liouville's theorem (Whittaker & Watson 1927, §20.12), the conjugate velocity field is thus given by an expression of the form

$$u - iv = \frac{d\bar{z}}{dt} = \frac{1}{2\pi i} \sum_{\beta=1}^{N} \Gamma_\beta \zeta(z - z_\beta; \omega_1, \omega_2) + C_N. \tag{2.2}$$

The overbar denotes complex conjugation. The term C_N is a constant as regards z, but it may depend on the geometry of the periodic domain, the vortex strengths, and the instantaneous vortex configuration.

The following arguments may be used to determine C_N. First, the dynamics of the particle motion governed by (2.2) consists of a superposition of contributions from each vortex, so that C_N may be written as a sum of N terms, each of which depends on the position of a single vortex. Next, note that the velocity of the particle due to

the presence of vortex β is proportional to the strength Γ_β. From these considerations C_N can be written as

$$C_N = \sum_{\beta=1}^{N} \Gamma_\beta f(z_\beta). \tag{2.3}$$

By spatial homogeneity the dynamics of the particle is also independent of the location of the coordinate origin, so that

$$\sum_{\beta=1}^{N} \Gamma_\beta f(z_\beta) = \sum_{\beta=1}^{N} \Gamma_\beta f(z_\beta - c) \tag{2.4}$$

for every complex number c. If c is taken to be the position of vortex α, with vortex α being any one of the N vortices, then

$$C_N = \sum_{\beta=1}^{N} \Gamma_\beta f(z_\beta) = \sum_{\beta=1}^{N}{}' \Gamma_\beta f(z_\beta - z_\alpha) + \Gamma_\alpha f(0)$$

$$= \sum_{\beta=1}^{N}{}' \Gamma_\beta \left[f(z_\beta - z_\alpha) - f(0) \right] = \sum_{\beta=1}^{N}{}' \Gamma_\beta g(z_\beta - z_\alpha), \tag{2.5}$$

with the prime on a sum indicating that the term $\beta = \alpha$ is excluded. Now consider the two-vortex problem with vortex strengths $\Gamma_1 = -\Gamma_2 = \Gamma$. In this case (2.5) gives

$$C_2 = -\Gamma g(z_1 - z_2) = \Gamma g(z_2 - z_1), \tag{2.6}$$

which demonstrates that g is an odd function. The constant in (2.2) for the three-vortex problem can be written as

$$C_3 = \Gamma_1 g(z_1 - z_3) + \Gamma_2 g(z_2 - z_3) = \Gamma_1 g(z_1 - z_2) + \Gamma_3 g(z_3 - z_2). \tag{2.7}$$

Since the sum of the vortex strengths is zero and g is an odd function, this expression for C_3 gives

$$g(z_1 - z_2) + g(z_2 - z_3) + g(z_3 - z_1) = 0, \tag{2.8a}$$

or

$$g(a) + g(b) = g(a + b) \tag{2.8b}$$

for arbitrary complex a, b. This equation is of the same form as Cauchy's functional equation for a real variable (Aczél 1969), which implies that g is linear in both the real and imaginary parts of its argument, i.e. $g(z)$ may be written as a linear function of z and $\bar{z}$. It follows from the linearity of g that f may be chosen as a linear function of both the real and imaginary parts of its argument; in particular, $f(0)$ may be chosen equal to zero, so that the additive constant in (2.2) can be written as (cf. (2.3))

$$C_N = \frac{1}{2\pi i} \sum_{\beta=1}^{N} \Gamma_\beta \left[A(\omega_1, \omega_2) z_\beta + B(\omega_1, \omega_2) \bar{z}_\beta \right]. \tag{2.9}$$

The constants A and B can now be determined using the invariance of the velocity field to period shifts in the vortex locations. If each base vortex at z_β in (2.2) is replaced by its periodic image at $z_\beta + 2m_\beta \omega_1 + 2n_\beta \omega_2$, with m_β and n_β arbitrary integers, this invariance requires that

$$\sum_{\beta=1}^{N} \Gamma_\beta \left[2m_\beta(\eta_1 - A\omega_1 - B\bar{\omega}_1) + 2n_\beta(\eta_2 - A\omega_2 - B\bar{\omega}_2) \right] = 0, \tag{2.10}$$

where $\eta_1 = \zeta(\omega_1)$ and $\eta_2 = \zeta(\omega_2)$. In writing (2.10) we have used the quasi-periodicity of the ζ-function:

$$\zeta(z + 2m\omega_1 + 2n\omega_2) = \zeta(z) + 2m\eta_1 + 2n\eta_2. \tag{2.11}$$

The factors multiplying m_β and n_β in (2.10) must vanish independently, giving two equations for A and B. The result of solving these is

$$A(\omega_1, \omega_2) = (\eta_1\bar{\omega}_2 - \eta_2\bar{\omega}_1) / (\omega_1\bar{\omega}_2 - \bar{\omega}_1\omega_2), \tag{2.12a}$$

$$B(\omega_1, \omega_2) = (\eta_2\omega_1 - \eta_1\omega_2) / (\omega_1\bar{\omega}_2 - \bar{\omega}_1\omega_2). \tag{2.12b}$$

Legendre's relation $\eta_1\omega_2 - \eta_2\omega_1 = \pi i/2$ allows us to write these constants as

$$A(\omega_1, \omega_2) = \frac{\eta_1}{\omega_1} - \frac{\pi\bar{\omega}_1}{\Delta\omega_1}, \quad B(\omega_1, \omega_2) = \frac{\pi}{\Delta}, \tag{2.13a}$$

where

$$\Delta = 2i(\omega_1\bar{\omega}_2 - \bar{\omega}_1\omega_2) \tag{2.13b}$$

is the area of the basic parallelogram.

Combining (2.2), (2.9) and (2.13a) gives the conjugate velocity of a passive particle at z in the field of N point vortices in a doubly periodic domain with half-periods ω_1 and ω_2 as

$$\frac{d\bar{z}}{dt} = \frac{1}{2\pi i} \sum_{\beta=1}^{N} \Gamma_\beta \left\{ \zeta(z - z_\beta; \omega_1, \omega_2) + \left(\frac{\eta_1}{\omega_1} - \frac{\pi\bar{\omega}_1}{\Delta\omega_1}\right) z_\beta + \frac{\pi}{\Delta}\bar{z}_\beta \right\}. \tag{2.14}$$

The linear impulse of the vortex system is given by

$$\sum_{\beta=1}^{N} \Gamma_\beta z_\beta = Q + iP, \tag{2.15}$$

so that the conjugate velocity field can be written as

$$\frac{d\bar{z}}{dt} = \frac{1}{2\pi i} \left\{ \sum_{\beta=1}^{N} \Gamma_\beta \zeta(z - z_\beta; \omega_1, \omega_2) + \left(\frac{\eta_1}{\omega_1} - \frac{\pi\bar{\omega}_1}{\Delta\omega_1}\right)(Q + iP) + \frac{\pi}{\Delta}(Q - iP) \right\}. \tag{2.16}$$

Note that the value of the linear impulse $Q + iP$ depends on which vortices are chosen as the base vortices. The resulting velocity field (2.16), however, is independent of the choice of base vortices, as it should be. Without loss of generality we may rotate our coordinates so that ω_1 lies along the x-axis, giving

$$\frac{d\bar{z}}{dt} = \frac{1}{2\pi i} \sum_{\beta=1}^{N} \Gamma_\beta \zeta(z - z_\beta; \omega_1, \omega_2) + \frac{\eta_1}{2\pi i\,\omega_1}(Q + iP) - \frac{P}{\Delta}. \tag{2.17}$$

The conjugate velocity of the vortex at z_α is now found by evaluating the limit

$$\frac{d\bar{z}_\alpha}{dt} = \lim_{z \to z_\alpha} \left(\frac{d\bar{z}}{dt} - \frac{1}{2\pi i} \frac{\Gamma_\alpha}{z - z_\alpha} \right). \tag{2.18}$$

Taking this limit in (2.17) gives the conjugate velocity of a vortex at z_α in the field of $N - 1$ point vortices in a doubly periodic domain with half-periods ω_1 and ω_2, with

ω_1 chosen to lie along the x-axis, as

$$\frac{d\bar{z}_\alpha}{dt} = \frac{1}{2\pi i}\sum_{\beta=1}^{N}{}'\Gamma_\beta\zeta(z_\alpha - z_\beta;\omega_1,\omega_2) + \frac{\eta_1}{2\pi i\,\omega_1}(Q + iP) - \frac{P}{\Delta}. \tag{2.19}$$

We have verified that for a square domain (2.19) agrees numerically with the results of Weiss & McWilliams (1991; equation (7)). We shall explore solutions of (2.19) for $N = 3$ and for different ratios of the vortex strengths and different shapes of the fundamental parallelogram.

Equation (2.19) can be written in Hamiltonian form as

$$\Gamma_\alpha\,dx_\alpha/dt = \partial H/\partial y_\alpha, \quad \Gamma_\alpha\,dy_\alpha/dt = -\partial H/\partial x_\alpha, \tag{2.20a,b}$$

with the Hamiltonian

$$H = -\frac{1}{2\pi}\sum_{\alpha=1}^{N}\sum_{\beta=\alpha+1}^{N}\Gamma_\alpha\Gamma_\beta\Bigg\{ \ln|\sigma(z_\alpha - z_\beta;\omega_1,\omega_2)|$$
$$-\mathrm{Re}\left[\frac{\eta_1}{2\omega_1}\left(z_\alpha - z_\beta\right)^2\right] - \frac{\pi}{\Delta}\left(y_\alpha - y_\beta\right)^2\Bigg\} \tag{2.21a}$$

given in terms of the Weierstrass σ-function (Whittaker & Watson 1927, §20.42), which is related to the ζ-function by $\zeta(z) = d\big(\log\sigma(z)\big)/dz$. This Hamiltonian can also be written in terms of the Jacobian ϑ_1-function (Whittaker & Watson 1927, chapter 21) as

$$H = -\frac{1}{2\pi}\sum_{\alpha=1}^{N}\sum_{\beta=\alpha+1}^{N}\Gamma_\alpha\Gamma_\beta\left\{\ln\left|2\omega_1\frac{\vartheta_1\big((z_\alpha - z_\beta)/2\omega_1\big)}{\vartheta_1{}'(0)}\right| - \frac{\pi}{\Delta}(y_\alpha - y_\beta)^2\right\}. \tag{2.21b}$$

Equations (2.21) agree, within an additive constant, with the Hamiltonian given by O'Neil (1989; equation (3.5)), which O'Neil states agrees numerically with the result of Campbell *et al.* (1989); this latter result agrees with that of Weiss & McWilliams (1991).

3. Solution method

Following the solution path from AS we use (2.15) and the vanishing of the sum of the circulations to write, for $N = 3$,

$$\Gamma_2(z_1 - z_2) + \Gamma_3(z_1 - z_3) = -(Q + iP), \tag{3.1a}$$

$$\Gamma_1(z_1 - z_2) - \Gamma_3(z_2 - z_3) = Q + iP, \tag{3.1b}$$

so that simple linear relations allow all three vortex separations to be expressed in terms of one, which we take to be†

$$z_1 - z_2 = Z. \tag{3.2a}$$

Thus,

$$\Gamma_3(z_1 - z_3) = -(Q + iP) - \Gamma_2 Z, \tag{3.2b}$$

$$\Gamma_3(z_2 - z_3) = -(Q + iP) + \Gamma_1 Z. \tag{3.2c}$$

† In AS this difference was denoted ζ; we use a different symbol here to avoid confusion with the Weierstrass ζ-function.

Without loss of generality we may assume that the labels of the vortices have been chosen such that $\Gamma_1 \geqslant \Gamma_2 > 0, \Gamma_3 < 0$, since two of the vortices must always have the same sign and the case of two negative vortices follows easily from the case of two positive vortices. As in AS we introduce the parameter γ such that

$$\Gamma_1/\Gamma_3 = -\left(\tfrac{1}{2} + \gamma\right), \tag{3.3a}$$

$$\Gamma_2/\Gamma_3 = -\left(\tfrac{1}{2} - \gamma\right), \tag{3.3b}$$

$$\Gamma_1/\Gamma_2 = (1 + 2\gamma)/(1 - 2\gamma). \tag{3.3c}$$

It follows from these relations that we cover the full range of parameters by allowing γ to vary between 0 and $\tfrac{1}{2}$.

From the equations of motion for the vortices (2.19), namely

$$\frac{\mathrm{d}\bar{z}_1}{\mathrm{d}t} = \frac{1}{2\pi\mathrm{i}} \left[\Gamma_2 \zeta(z_1 - z_2) + \Gamma_3 \zeta(z_1 - z_3)\right] + \frac{\eta_1}{2\pi\mathrm{i}\,\omega_1}(Q + \mathrm{i}P) - \frac{P}{\Delta}, \tag{3.4a}$$

$$\frac{\mathrm{d}\bar{z}_2}{\mathrm{d}t} = \frac{1}{2\pi\mathrm{i}} \left[\Gamma_1 \zeta(z_2 - z_1) + \Gamma_3 \zeta(z_2 - z_3)\right] + \frac{\eta_1}{2\pi\mathrm{i}\,\omega_1}(Q + \mathrm{i}P) - \frac{P}{\Delta}, \tag{3.4b}$$

$$\frac{\mathrm{d}\bar{z}_3}{\mathrm{d}t} = \frac{1}{2\pi\mathrm{i}} \left[\Gamma_1 \zeta(z_3 - z_1) + \Gamma_2 \zeta(z_3 - z_2)\right] + \frac{\eta_1}{2\pi\mathrm{i}\,\omega_1}(Q + \mathrm{i}P) - \frac{P}{\Delta}, \tag{3.4c}$$

we obtain for Z the equation of motion

$$\frac{\mathrm{d}\bar{Z}}{\mathrm{d}t} = -\frac{\Gamma_3}{2\pi\mathrm{i}} \left\{\zeta(z_1 - z_2) + \zeta(z_2 - z_3) + \zeta(z_3 - z_1)\right\}$$

$$= -\frac{\Gamma_3}{2\pi\mathrm{i}} \left\{\zeta(Z) + \zeta\left(X - (\tfrac{1}{2} + \gamma)Z\right) - \zeta\left(X + (\tfrac{1}{2} - \gamma)Z\right)\right\}, \tag{3.5}$$

where

$$X = -\frac{Q + \mathrm{i}P}{\Gamma_3}. \tag{3.6}$$

In (3.4) and (3.5) the Weierstrass ζ-function has half-periods ω_1 and ω_2. Equation (3.5) is the counterpart of the equation for the relative position of vortices 1 and 2 derived for the case of three vortices of vanishing total circulation in a periodic strip (AS, equation (2.5)). Analogously to our treatment of that equation we seek an interpretation of (3.5) in terms of the advection of a fictitious passive particle at Z by a system of fixed vortices.

To this end let us consider the position and nature of the singularities of the function on the right-hand side of (3.5). First, the term $-\Gamma_3\zeta(Z)/2\pi\mathrm{i}$ has a lattice of poles at $\Omega_{mn} = 2m\omega_1 + 2n\omega_2$, $m, n = 0, \pm 1, \ldots$, with each pole having residue $-\Gamma_3/2\pi\mathrm{i}$. Next, the term $-\Gamma_3\zeta\left[X - (\tfrac{1}{2} + \gamma)Z\right]/2\pi\mathrm{i}$ has a lattice of poles at $(\Omega_{mn} + X)/(\tfrac{1}{2} + \gamma)$, $m, n = 0, \pm 1, \ldots$, with each having residue $\Gamma_3/[2\pi\mathrm{i}(\tfrac{1}{2} + \gamma)] = -\Gamma_3{}^2/(2\pi\mathrm{i}\Gamma_1)$. This can be seen by noting that the identity (Whittaker & Watson 1927, §20.4)

$$\zeta(z; \omega_1, \omega_2) = L\zeta(Lz; L\omega_1, L\omega_2) \tag{3.7}$$

allows us to write the second term in (3.5) as

$$\zeta\left(X - (\tfrac{1}{2} + \gamma)Z; \omega_1, \omega_2\right) = -\frac{1}{\tfrac{1}{2} + \gamma}\, \zeta\left(Z - \frac{X}{\tfrac{1}{2} + \gamma}; \frac{\omega_1}{\tfrac{1}{2} + \gamma}, \frac{\omega_2}{\tfrac{1}{2} + \gamma}\right). \tag{3.8}$$

Finally, by a similar transformation, we see that the term $\Gamma_3\zeta\left[X + (\tfrac{1}{2} - \gamma)Z\right]/2\pi\mathrm{i}$ has

a lattice of poles at $(\Omega_{mn} - X)/(\frac{1}{2} - \gamma)$, $m, n = 0, \pm 1, \ldots$, with each having residue $\Gamma_3/[2\pi\mathrm{i}(\frac{1}{2}-\gamma)] = -\Gamma_3{}^2/(2\pi\mathrm{i}\Gamma_2)$. If γ is rational, and equal to p/q in lowest terms, these three lattices of poles are all periodic with half-periods $2q\omega_1$ and $2q\omega_2$. There are $6q^2+8p^2$ poles within a parallelogram with these half-periods: $(2q)^2$ poles with residue $-\Gamma_3/2\pi\mathrm{i}$ at $\Omega_{mn} = 2m\omega_1 + 2n\omega_2$ for $m, n = 0, 1, \ldots, 2q-1$; $(q+2p)^2$ poles with residue $2q\Gamma_3/2\pi\mathrm{i}(q+2p)$ at $2q(X+\Omega_{mn})/(q+2p)$, $m, n = 0, 1, \ldots, q+2p-1$; and $(q-2p)^2$ poles with residue $2q\Gamma_3/2\pi\mathrm{i}(q - 2p)$ at $-2q(X - \Omega_{mn})/(q - 2p)$, $m, n = 0, 1, \ldots, q - 2p - 1$. Note that the sum of the residues of these poles is zero; thus, for rational γ, (3.5) is an elliptic function with half-periods $2q\omega_1$ and $2q\omega_2$. Also notice that, depending on the value of X, not all of the above poles will lie within the fundamental parallelogram.

By Liouville's theorem, it follows from these considerations that

$$\zeta(Z; \omega_1, \omega_2) + \zeta\left(X - \frac{2p+q}{2q} Z; \omega_1, \omega_2\right) - \zeta\left(X + \frac{2p-q}{2q} Z; \omega_1, \omega_2\right)$$

$$= \sum_{m,n=0}^{2q-1} \zeta\left(Z - \Omega_{mn}; 2q\omega_1, 2q\omega_2\right)$$

$$- \frac{2q}{q+2p} \sum_{m,n=0}^{q+2p-1} \zeta\left(Z - \frac{2q(X + \Omega_{mn})}{q + 2p}; 2q\omega_1, 2q\omega_2\right)$$

$$- \frac{2q}{q-2p} \sum_{m,n=0}^{q-2p-1} \zeta\left(Z + \frac{2q(X - \Omega_{mn})}{q - 2p}; 2q\omega_1, 2q\omega_2\right) + \text{constant.} \quad (3.9)$$

The ζ-functions on the left-hand side have half-periods ω_1 and ω_2, since they originate from the 'physical' period-parallelogram, whereas the ζ-functions on the right-hand side have half-periods $2q\omega_1$ and $2q\omega_2$, as introduced by the consideration of singularities and their periodicity.

3.1. *A digression on velocities*

In order to evaluate the constant in (3.9) we pause to pursue the following problem. Consider a periodic array of vortices produced by two vortices with circulations $+\Gamma$ and $-\Gamma$ located at z_1 and z_2, respectively, in a parallelogram with half-periods ω_1 and ω_2. The velocity of vortex 1 is given by (2.19) as

$$\frac{\mathrm{d}\bar{z}_1}{\mathrm{d}t} = -\frac{\Gamma}{2\pi\mathrm{i}}\zeta(z_1 - z_2; \omega_1, \omega_2) + \frac{1}{2\pi\mathrm{i}}\frac{\eta_1}{\omega_1}(Q + \mathrm{i}P) - \frac{P}{\Delta}. \quad (3.10)$$

Now, imagine calculating this velocity using an $L \times L$ piece of the above vortex array in a parallelogram with half-periods $L\omega_1$ and $L\omega_2$, where L is an integer. According to (2.19) the result is

$$\frac{\mathrm{d}\bar{z}_1}{\mathrm{d}t} = \frac{\Gamma}{2\pi\mathrm{i}} \sum_{m,n=0}^{L-1}{}' \zeta\left(z_1 - (z_1 + \Omega_{mn}); L\omega_1, L\omega_2\right)$$

$$- \frac{\Gamma}{2\pi\mathrm{i}} \sum_{m,n=0}^{L-1} \zeta\left(z_1 - (z_2 + \Omega_{mn}); L\omega_1, L\omega_2\right) + \frac{1}{2\pi\mathrm{i}}\frac{\zeta(L\omega_1; L\omega_1, L\omega_2)}{L\omega_1}L^2(Q + \mathrm{i}P) - \frac{L^2 P}{L^2 \Delta},$$

$$(3.11)$$

with the prime on the first sum again indicating that the singular term $(m, n) = (0, 0)$ is omitted. The conjugate velocity of vortex 1 must, of course, be the same in the two

representations. Thus, comparing expressions (3.10) and (3.11), we have the result

$$\zeta(Z\,;\omega_1,\omega_2) = \sum_{m,n=0}^{L-1} \zeta(Z - \Omega_{mn}; L\omega_1, L\omega_2) + \sum_{m,n=0}^{L-1}{}' \zeta(\Omega_{mn}; L\omega_1, L\omega_2), \qquad (3.12)$$

where we have substituted Z for the arbitrary value of $z_1 - z_2$.

The second sum in (3.12) is performed by first using the identity (3.7) to write the summand as $(1/L)\zeta(\Omega_{mn}/L;\omega_1,\omega_2)$. Now we split the sum into three: one for $m = 0$, one for $n = 0$, and one over $1 \leqslant m, n \leqslant L - 1$. In the first of these we perform the sum by adding pairs of terms $\zeta(\Omega_{0n}/L;\omega_1,\omega_2) = \zeta(2n\omega_2/L;\omega_1,\omega_2)$ such that their arguments add to ω_2. If L is odd, there are $(L-1)/2$ such pairs. If L is even, there are $L/2 - 1$ such pairs and a term η_2 'left over'. In either case, according to the addition theorem for the ζ-function (2.11), each pair contributes $2\eta_2$ to the sum, and the result of the sum with $m = 0$ is $(L-1)\eta_2/L$. In exactly the same way it is seen that the sum with $n = 0$ is $(L-1)\eta_1/L$.

For the sum over the bulk of the points, $1 \leqslant m, n \leqslant L - 1$, we pair off terms such that the arguments add to $\omega_3 = \omega_1 + \omega_2$. For even L there are $(L-1)^2/2$ such pairs, each contributing $2\eta_3 = 2\zeta(\omega_3;\omega_1,\omega_2)$ to the sum. For odd L there are $[(L-1)^2-1]/2$ pairs, each contributing $2\eta_3$ to the sum, and a single term η_3 'left over' (corresponding to $m = n = (L-1)/2$). In either case the resulting sum is $\eta_3(L-1)^2/L$.

Finally, using $\eta_3 = \eta_1 + \eta_2$, we have the result

$$\sum_{m,n=0}^{L-1}{}' \zeta(\Omega_{mn}; L\omega_1, L\omega_2) = \frac{L-1}{L}(\eta_1 + \eta_2 + (L-1)\eta_3) = (L-1)\eta_3. \qquad (3.13)$$

Substituting this into (3.12) we have

$$\zeta(Z\,;\omega_1,\omega_2) = \sum_{m,n=0}^{L-1} \zeta(Z - \Omega_{mn}; L\omega_1, L\omega_2) + (L-1)\,\zeta(\omega_3;\omega_1,\omega_2), \qquad (3.14)$$

which allows us to write a ζ-function on a period-parallelogram with half-periods ω_1 and ω_2 as a sum of ζ-functions with half-periods $L\omega_1$ and $L\omega_2$ for any integer L. In AS an analogous result was found for the cotangent function, which can be obtained from (3.14) by taking the limit to a singly periodic domain.

We now return to (3.9) to determine the constant on the right-hand side. From (3.14), the first sum on the right-hand side of (3.9) can be written as

$$\sum_{m,n=0}^{2q-1} \zeta(Z - \Omega_{mn}; 2q\omega_1, 2q\omega_2) = \zeta(Z\,;\omega_1,\omega_2) - (2q - 1)\,\zeta(\omega_3;\omega_1,\omega_2). \qquad (3.15a)$$

The second sum on the right-hand side of (3.9) requires a bit more work. It can be written as

$$r \sum_{m,n=0}^{q+2p-1} \zeta\big(Z - r(X + \Omega_{mn}); 2q\omega_1, 2q\omega_2\big)$$

$$= r \sum_{m,n=0}^{q+2p-1} \zeta\big(r(Z/r - X - \Omega_{mn}); (q + 2p)r\omega_1, (q + 2p)r\omega_2\big)$$

$$= \sum_{m,n=0}^{q+2p-1} \zeta\big(Z/r - X - \Omega_{mn}; (q + 2p)\omega_1, (q + 2p)\omega_2\big)$$

$$= \zeta(Z/r - X;\omega_1,\omega_2) - (q + 2p - 1)\,\zeta(\omega_3;\omega_1,\omega_2), \qquad (3.15b)$$

with $r = 2q/(q + 2p)$. Similarly, the last sum in (3.9) can be written as

$$\frac{2q}{q-2p} \sum_{m,n=0}^{q-2p-1} \zeta\left(Z + \frac{2q(X - \Omega_{mn})}{q-2p}; 2q\omega_1, 2q\omega_2\right)$$

$$= \zeta\left(\frac{q-2p}{2q}Z + X; \omega_1, \omega_2\right) - (q - 2p - 1)\,\zeta(\omega_3; \omega_1, \omega_2). \quad (3.15c)$$

Combining (3.15) we find that the constant in (3.9) is $\eta_3 = \zeta(\omega_3; \omega_1, \omega_2)$.

3.2. Interpretation as an advection problem

We now wish to compare (3.5) to the equation of motion for a passive particle at Z in the field of a certain periodic system of fixed vortices in a parallelogram with half-periods $2q\omega_1$ and $2q\omega_2$. These vortices are, of course, precisely the singularities discussed just before (3.9) above. We recall that they come from one of three 'families': $(2q)^2$ vortices of circulation $-\Gamma_3$ at $\Omega_{mn} = 2m\omega_1 + 2n\omega_2$, $m, n = 0, 1, \ldots, 2q - 1$; $(q + 2p)^2$ of circulation $2q\Gamma_3/(q + 2p) = -\Gamma_3{}^2/\Gamma_1$ at $2q(X + \Omega_{mn})/(q + 2p)$, $m, n = 0, 1, \ldots, q + 2p - 1$; and $(q - 2p)^2$ of circulation $2q\Gamma_3/(q - 2p) = -\Gamma_3{}^2/\Gamma_2$ at $-2q(X - \Omega_{mn})/(q - 2p)$, $m, n = 0, 1, \ldots, q - 2p - 1$. This system of $6q^2 + 8p^2$ vortices is quite interesting independently of its relation to the original three-vortex problem. A calculation of the velocity of any vortex in such a configuration due to the effects of the remaining vortices reveals that these three families of vortices form a stationary lattice. As illustrated in figure 12, these configurations quickly become very complicated. In fact, as we shall see in more detail in §6, an irrational value of γ corresponds to a stationary vortex configuration that is aperiodic!

Using the form of the velocity field from (2.16), we can write the equation of motion for a passively advected particle at Z as

$$\frac{\mathrm{d}\bar{Z}}{\mathrm{d}t} = -\frac{\Gamma_3}{2\pi\mathrm{i}} \left\{ \sum_{m,n=0}^{2q-1} \zeta(Z - \Omega_{mn}; 2q\omega_1, 2q\omega_2) \right.$$

$$- \frac{2q}{q+2p} \sum_{m,n=0}^{q+2p-1} \zeta\left(Z - \frac{2q(X + \Omega_{mn})}{q+2p}; 2q\omega_1, 2q\omega_2\right)$$

$$\left. - \frac{2q}{q-2p} \sum_{m,n=0}^{q-2p-1} \zeta\left(Z + \frac{2q(X - \Omega_{mn})}{q-2p}; 2q\omega_1, 2q\omega_2\right) \right\}$$

$$- \frac{1}{2\pi\mathrm{i}} \left[\frac{\pi}{(2q)^2 \Delta} \frac{2q\bar{\omega}_1}{2q\omega_1} - \frac{\zeta(2q\omega_1; 2q\omega_1, 2q\omega_2)}{2q\omega_1}\right] (Q + \mathrm{i}P) + \frac{1}{2\pi\mathrm{i}} \frac{\pi}{(2q)^2\Delta} (Q - \mathrm{i}P),$$

$$(3.16)$$

where Δ is the area of the basic parallelogram in real space and Q and P are the components of the impulse for the system of $6q^2 + 8p^2$ vortices:

$$Q + \mathrm{i}P = -\Gamma_3 \left[\sum_{m,n=0}^{2q-1} \Omega_{mn} - \frac{2q}{q+2p} \sum_{m,n=0}^{q+2p-1} \frac{2q(X + \Omega_{mn})}{q+2p}\right.$$

$$\left. + \frac{2q}{q-2p} \sum_{m,n=0}^{q-2p-1} \frac{2q(X - \Omega_{mn})}{q-2p}\right] = -(2q)^2\Gamma_3\omega_3. \quad (3.17)$$

The last two terms on the right-hand side of (3.16) now become

$$-\frac{\Gamma_3}{2\pi i\omega_1}\left[\eta_1\omega_3 + \frac{\pi}{\Delta}(\omega_1\bar{\omega}_3 - \bar{\omega}_1\omega_3)\right] = -\frac{\Gamma_3}{2\pi i}\left[\eta_1 + \frac{1}{\omega_1}\left(\eta_1\omega_2 - \frac{i\pi}{2}\right)\right] = -\frac{\Gamma_3\eta_3}{2\pi i},$$

(3.18)

where the last step uses Legendre's relation $\eta_1\omega_2 - \eta_2\omega_1 = i\pi/2$. Thus, the equation of motion for a passively advected particle at Z can be written as

$$\frac{d\bar{Z}}{dt} = -\frac{\Gamma_3}{2\pi i}\left\{\sum_{m,n=0}^{2q-1}\zeta(Z - \Omega_{mn}; 2q\omega_1, 2q\omega_2)\right.$$

$$-\frac{2q}{q+2p}\sum_{m,n=0}^{q+2p-1}\zeta\left(Z - \frac{2q(X+\Omega_{mn})}{q+2p}; 2q\omega_1, 2q\omega_2\right)$$

$$\left. -\frac{2q}{q-2p}\sum_{m,n=0}^{q-2p-1}\zeta\left(Z + \frac{2q(X-\Omega_{mn})}{q-2p}; 2q\omega_1, 2q\omega_2\right) + \eta_3\right\}.$$

(3.19)

According to (3.9) and the evaluation of the constant in that equation accomplished in §3.1, we see that (3.19) reduces to (3.5). In other words, we have shown, for rational γ, that the evolution of the relative position of vortices 1 and 2 in the original, periodic three-vortex problem can be identified with the passive advection of a fictitious particle by a certain system of stationary point vortices in a larger, periodic parallelogram similar to the original periodic domain. To facilitate differentiating between the original three-vortex system and this stationary vortex system, we refer to the domain of the original vortices as 'real space' and the domain of the stationary vortices as 'phase space'.

The problem of advection by stationary point vortices defines a Hamiltonian system. Taking $Z = x + iy$, (3.19) can be written as

$$dx/dt = \partial H/\partial y, \quad dy/dt = -\partial H/\partial x,$$

(3.20a,b)

with an appropriate choice for the Hamiltonian H. For computational purposes it is convenient to work with the form of the conjugate velocity field in (3.5), which gives

$$H = \frac{\Gamma_3}{2\pi}\left\{\ln|\sigma(Z)| - \frac{1}{\frac{1}{2}+\gamma}\ln|\sigma((\tfrac{1}{2}+\gamma)Z - X)| - \frac{1}{\frac{1}{2}-\gamma}\ln|\sigma((\tfrac{1}{2}-\gamma)Z + X)|\right\}.$$

(3.21)

This system is, of course, integrable. The determination of individual vortex motions in real space requires one additional quadrature, and this problem is thus also integrable, as already mentioned. We use the following procedure to determine the real-space vortex trajectories. Level curves of H (3.21) give streamlines in phase space; from these streamlines and (3.19) it is possible to numerically determine $Z(t)$. The equation of motion for z_1 (3.4a) can be written in terms of Z as

$$\frac{d\bar{z}_1}{dt} = \frac{1}{2\pi i}\left[\Gamma_2\zeta(Z) + \Gamma_3\zeta((\tfrac{1}{2}-\gamma)Z + X)\right] + \frac{\eta_1}{2\pi i\,\omega_1}(Q + iP) - \frac{P}{\Delta},$$

(3.22)

so that once $Z(t)$ is known, $z_1(t)$ is determined by numerical quadrature. Vortex positions $z_2(t)$ and $z_3(t)$ are then given by (3.2).

With the general framework established, at least for rational γ, we turn to a study of special cases that have been selected to be somewhat representative. A comprehensive parametric study is not possible here, since we are dealing with at

least five independent system parameters: the shape of the basic parallelogram as determined by ω_1 and ω_2; the ratio of vortex circulations, γ; and the parameter X in (3.6) containing two components of the system impulse Q and P. As for the case of the periodic strip studied in AS we shall find it convenient to specify the shape of the periodic domain and the value of γ, and then to explore variations in X rather fully, with 'representative' values of X singled out for further detailed study of vortex trajectories.

4. The special case $\gamma = 0$ ($\Gamma_1 = \Gamma_2$)

Choosing $\gamma = 0$ gives the simplest possible ratio of vortex strengths, $\Gamma_1 : \Gamma_2 : \Gamma_3 = 1 : 1 : (-2)$. From (3.5) the advection equation to be solved in this case is

$$\frac{\mathrm{d}\bar{Z}}{\mathrm{d}t} = -\frac{\Gamma_3}{2\pi\mathrm{i}} \left\{ \zeta(Z) + \zeta\left(X - \tfrac{1}{2}Z\right) - \zeta\left(X + \tfrac{1}{2}Z\right) \right\}. \tag{4.1}$$

In our formulation above this corresponds to $p = 0$ and $q = 1$. Thus, from (3.19) the equation of motion can be written as

$$\frac{\mathrm{d}\bar{Z}}{\mathrm{d}t} = -\frac{\Gamma_3}{2\pi\mathrm{i}} \left\{ \sum_{m,n=0}^{1} \zeta(Z - \Omega_{mn}; 2\omega_1, 2\omega_2) \right.$$

$$\left. - 2\zeta(Z - 2X; 2\omega_1, 2\omega_2) - 2\zeta(Z + 2X; 2\omega_1, 2\omega_2) + \eta_3 \right\}, \tag{4.2}$$

and the advection problem for Z takes place in a periodic parallelogram with half-periods $2\omega_1$ and $2\omega_2$, which is twice the size of the real-space parallelogram. In general there are six stationary vortices generating the advecting flow (along with their periodic images): four of circulation $-\Gamma_3$ located at $z = 0$, $2\omega_1$, $2\omega_2$, and $2\omega_1 + 2\omega_2$, and two of circulation $2\Gamma_3$ at $\pm 2X$.

4.1. *The simplest case: $X = 0$ in a square domain*

A particularly simple case arises if $X = 0$ and the real space domain is a square. Here, as in the remainder of the paper, we use the notation $L = 2\omega_1$ to denote the width of the fundamental parallelogram in real space. According to (3.2) we have $z_3 - z_1 = -(z_3 - z_2)$, and (3.4c) then shows that vortex 3 remains stationary. In the advection problem the vortex at the origin† has circulation $3\Gamma_3$, and there are three other advecting vortices of circulation $-\Gamma_3$ at $2\omega_1$, $2\omega_2$, and $2\omega_1 + 2\omega_2$, respectively. The pattern of the advected particle paths (or, equivalently, streamlines) in the steady flow produced by these four fixed vortices is shown in the phase-space diagram of figure 1. All streamlines shown are separatrices or 'dividing streamlines', i.e. they connect stagnation points of the advection problem. There are four regimes of motion in figure 1 labelled I, II, III and IV. As in AS, regimes of motion are designated by Roman numerals and motions along separatrices by lower-case Greek letters. For this simple case the motion is always bounded, in the sense that $|Z|$ is bounded. The top four panels of figure 2 display typical trajectories of the base vortices for each of the four regimes in figure 1 according to the labels indicated. For all of these motions, vortices 1 and 2 move periodically along the indicated trajectories and vortex 3 remains stationary. The bottom four panels of figure 2 correspond to

---

† This vortex at the origin arises by the coalescence of the two vortices of circulation $2\Gamma_3$ at $\pm 2X$ with the vortex of circulation $-\Gamma_3$, which is always present at the origin.
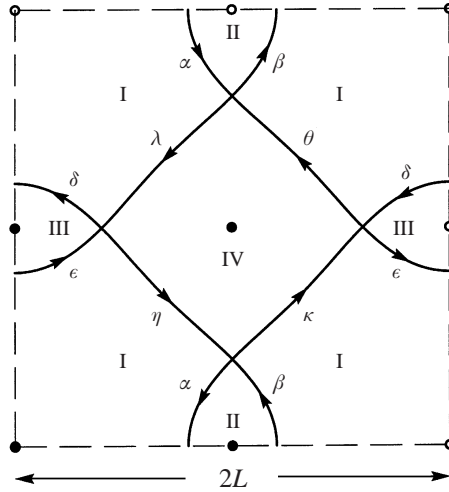
FIGURE 1. Phase space in a square domain for $\gamma = 0$, or $\Gamma_1 : \Gamma_2 : \Gamma_3 = 1 : 1 : (-2)$, and $X = 0$. The sides of the square are $2L$ and there are four stationary vortices (solid dots). The four regimes of motion are labelled I–IV and the eight separatrices α–λ.
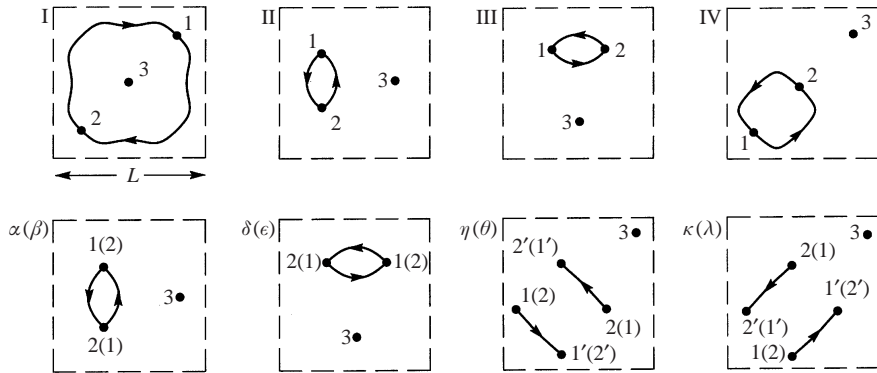

FIGURE 2. Real-space trajectories of the three vortices in a square domain with sides of length L for $\gamma = X = 0$ corresponding to the phase-space diagram of figure 1. Vortex 3 is stationary in all cases. All motions are shown for one period (in the case of separatrices, for the transition from saddle to saddle). The motions in β, ϵ, θ, and λ are obtained by interchanging vortices 1 and 2 in α, δ, η, and κ respectively.

motions along the eight separatrices in figure 1. The motions along the separatrices α, β, δ, and ϵ consist of vortices 1 and 2 switching places in infinite time. Motion along separatrix β, for example, looks exactly like motion along separatrix α except that the numbering of vortices 1 and 2 is interchanged, which is indicated by the parenthetical numbering in figure 2. Motions along the separatrices η, θ, κ, and λ consist of vortices 1 and 2 moving to the positions marked $1'$, $2'$ in infinite time. The conventions used in figure 2 (and later in other trajectory plots) are that the original base vortices are indicated by solid circles; initial vortex positions are given by the numbers 1, 2, and 3; and final positions by $1'$, $2'$, and $3'$ when vortex 3 moves.

4.2. *Bifurcations for $X \neq 0$ and a square domain*

The simple picture that emerges for $X = 0$ is immediately complicated when $X \neq 0$. Figure 3, for example, shows the advecting vortex system and its streamlines for
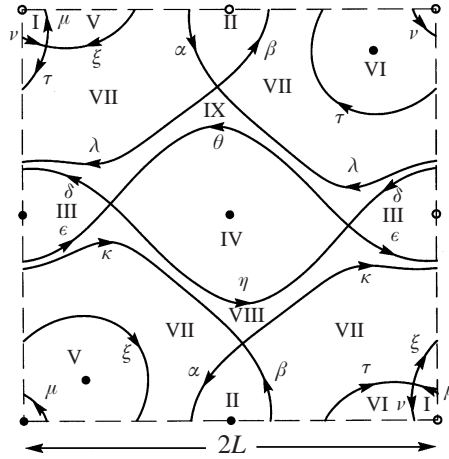
FIGURE 3. Phase space in a square domain for $\Gamma_1 : \Gamma_2 : \Gamma_3 = 1 : 1 : (-2)$, or $\gamma = 0$, and a non-degenerate value of $X = L(0.3 + i0.2)/2$ (point (*i*) on the bifurcation diagram of figure 5). The sides of the square are $2L$ and there are now six stationary vortices (solid dots). There are nine regimes labelled I–IX and twelve separatrices labelled α–τ.

$X = L(0.3 + i0.2)/2$. Now all six advecting vortices are present, giving nine regimes of motion. Three of these regimes yield qualitatively new motions of the advected particle. In regime VII the particle at Z orbits several of the stationary vortices instead of just one. In regimes VIII and IX the motion of the particle at Z is unbounded, in the sense that $|Z|$ is unbounded, when viewing the square domain in figure 3 as one tile in the complex plane. Thus the distance between vortices 1 and 2 is unbounded, and, according to (3.2), when vortices 1 and 2 separate, all three vortices will separate; i.e. although they all start in the same period-parallelogram, any two of the vortices will over time migrate farther and farther apart so that these base vortices are eventually separated by many periods. There are, of course, periodic images in each parallelogram, but the effect remains that considerable interchange occurs among parallelograms in this case.

The top seven panels of figure 4 show sample vortex trajectories in real space for each of the nine regimes of figure 3. The conventions used in figure 4 are that the original base vortices are indicated by solid circles; image vortices are indicated by open circles; initial vortex positions are given by the numbers 1, 2, and 3; final positions by 1′, 2′, and 3′; and regimes with the same motion but with the labelling of vortices 1 and 2 interchanged are indicated by parenthetical numbering. In the initial and final configurations we also join the vortices by a triangle to more clearly illustrate how the vortex configuration re-emerges after one period of the relative motion (or how a steady state at one end of a separatrix arises from the steady state at the other end). In some cases, such as in regimes VIII and IX, showing the motion of periodic images is essential for understanding how this re-emergence comes about. In these cases the trajectories of the required periodic images are shown by light lines with the initial and final vortex positions indicated by open circles and the final positions numbered 1″, 2″, or 3″.

Notice that the trajectories from regimes I, II, III, and IV in figure 4 are similar to those of figure 2 in that vortices 1 and 2 orbit as a pair, although here there is a net translation of the vortex configuration. We term vortex motions in these regimes *paired motions* since they consist of two like-sign vortices orbiting in close proximity.
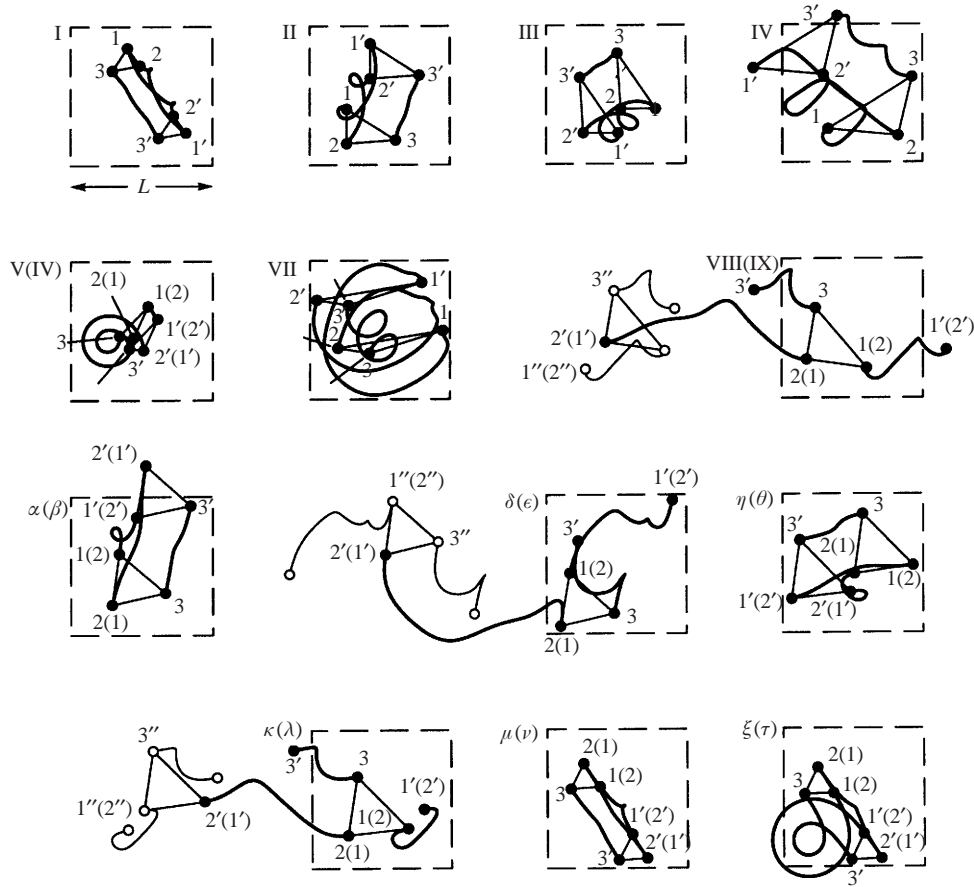
FIGURE 4. Real-space trajectories of the three vortices with $\gamma = 0$ and $X = L(0.3 + \mathrm{i}0.2)/2$ corresponding to the nine regimes and twelve separatrices of the phase-space diagram in figure 3.

Trajectories from regimes V and VI are also similar, but now the pairing is between either vortices 1 and 3 or vortices 2 and 3. Since the pairs now contain vortices of opposite sign we term vortex motions in these regimes *coupled motions*. Regime VII, in which the particle at Z orbits several of the stationary vortices, yields vortex motion in real space with vortices 1, 2, and 3 all interacting. This type of motion we term *collective motion*. Finally, motions from regimes VIII and IX, which behave as described above with $|Z|$ unbounded, we term *wandering motions*.

Vortex trajectories corresponding to motions along the separatrices of figure 3 are shown in the bottom six panels of figure 4. It can be seen here that the separatrix motions contain much of the information needed to construct the motions in the adjacent regimes. For example, the motion in panel II of figure 4 is a 'combination' of the separatrix motions α and β, as would be expected from figure 3. Similarly, the motion in regime VIII resembles the motion corresponding to the separatrix κ. It is important to remember, however, that the motions within regimes are truly periodic, whereas the separatrix motions are not periodic but begin and end at a steady state (which must be unstable). The extent in real space of a separatrix motion as displayed in our figures is somewhat arbitrary, since it can be continued 'forever' both before and after the segment shown.

Different values of X give different streamline configurations in phase space. In

general a streamline pattern for $\gamma = 0$ will look similar to that of figure 3 in that stagnation points of the flow will be joined together pairwise by the separating streamlines. However, as illustrated in figure 1 with $X = 0$, there are certain values of the impulse for which the streamline pattern is *degenerate*, with several of the stagnation points being joined together by separatrices. A complete discussion of the variability of the streamline patterns with X leads us to a bifurcation analysis.

Before pursuing such a bifurcation analysis, it is necessary to determine the range of X that we need to investigate. We have stressed the notion of 'base vortices' from which the entire vortex lattice can be constructed by periodic continuation. However, the dynamic problem is invariant to a shift of the 'base' vortex by an integral number of periods, i.e. simultaneous shifts of z_1, z_2, and z_3 by integral multiples of $2\omega_1$ or $2\omega_2$ in the original setup lead to the same problem. This means that changing X by $2\omega_1[(\frac{1}{2} + \gamma)m_1 + (\frac{1}{2} - \gamma)m_2 - m_3] + 2\omega_2[(\frac{1}{2} + \gamma)n_1 + (\frac{1}{2} - \gamma)n_2 - n_3]$, where m_j and n_j, $j = 1, 2, 3$, are integers, leads to the same problem. The smallest possible non-zero multiples of the periods that this expression can assume are $2(\frac{1}{2} - \gamma)\omega_1$ and $2(\frac{1}{2} - \gamma)\omega_2$. Hence, it is only necessary to consider values of X in a parallelogram with half-periods $(\frac{1}{2} - \gamma)\omega_1$ and $(\frac{1}{2} - \gamma)\omega_2$. We emphasize that the values of X are not periodic, but changing the value of X by integer multiples of $2(\frac{1}{2} - \gamma)\omega_1$ and $2(\frac{1}{2} - \gamma)\omega_2$ leads to the same dynamical problem.

The results of the bifurcation analysis for $\gamma = 0$ and a square domain are shown in figure 5. In the bottom right corner we show the bifurcation diagram in the X-plane, with the values of X restricted to a square with sides of length $L/2$. Panels (a–h) show representative streamline patterns in phase space, periodic in a square with sides $2L$. Values of X for which the streamline patterns are degenerate are indicated by the solid curves in the bifurcation diagram. For example, point (a) corresponds to $X = 0$ and leads to the streamline pattern shown both in figure 1 and panel (a) of figure 5. For this value of X each stagnation point is joined to every other stagnation point (or a periodic image). If we increase the value of X along the diagonal bifurcation line to point (d), we arrive at the streamline pattern in panel (d). Since point (d) lies on the same bifurcation line as point (a), we see a similar degeneracy in the streamline pattern, although all six stationary vortices are present in panel (d). Increasing the value of X further along the bifurcation line to point (h), with $X = L(1 + \mathrm{i})/4$, we reach an interesting degeneracy. At this value of X all of the bifurcation lines intersect, so that in the streamline plot all of the stagnation points are connected to each other by separatrices. In fact, as shown in panel (h) of figure 5, there are now only two stagnation points, each joined to the other (or a periodic image) by eight separatrices. Note that any value of X along the diagonal bifurcation line corresponds to a streamline pattern in which the motion of the particle at Z is bounded in every regime. Changing the value of X to that at point (i) leads to the non-degenerate streamline pattern shown in figure 3. The other non-degenerate examples shown are those with X values corresponding to points (b) and (c). Comparing figure 3 and panel (b) of figure 5 shows that X-values from the same regime in the bifurcation diagram correspond to qualitatively similar streamline patterns.

A closer examination of the streamline patterns resulting from different X values shows that the eight regimes in the bifurcation diagram of figure 5 do not represent eight unique sets of streamline patterns. For example, the pattern in panel (b) of figure 5, with $X = L/8$, is a 90° rotation of the pattern in panel (c) with $X = \mathrm{i}L/8$. Similarly, the pattern in panel (e) is a 90° rotation of the pattern in panel (g). Thus, for this case of $\gamma = 0$ in a square domain, it is necessary to examine only values of X from one of the triangles formed by the bifurcation lines; the streamline pattern
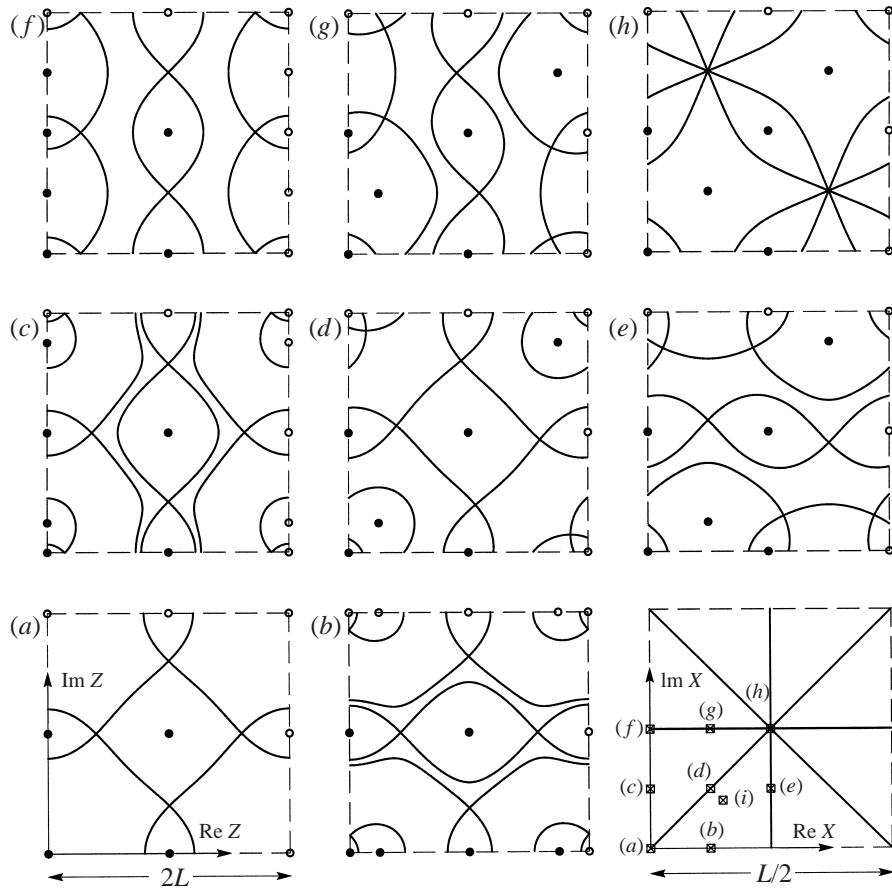
FIGURE 5. Bifurcation diagram in X-space (lower right) and representative streamline patterns in the field of the stationary phase-space vortices (panels $(a$–$h)$) for $\Gamma_1 : \Gamma_2 : \Gamma_3 = 1 : 1 : (-2)$, or $\gamma = 0$, and a square domain. The phase-space diagram corresponding to point (i) in the bifurcation diagram is shown in figure 3.

corresponding to any other value of X can be obtained by rotating, reflecting, or shifting the origin of a streamline pattern corresponding to a value of X from this triangle. Furthermore, as we noted above, only one value of X needs to be examined from the interior of the triangle as any other value of X in the interior provides a qualitatively similar streamline pattern. As a result, figure 5 provides a fairly complete description of the entire phase space for this choice of parameters.

4.3. *Domains that are not square*

The results of §§ 4.1 and 4.2 are complicated further when we consider domains that are not square. Varying the parallelogram shape consists of changing the aspect ratio $a = |\omega_2|/|\omega_1|$ and/or the angle φ between the half-periods ω_1 and ω_2. Here we only present results of varying one or the other of these two parameters.

Figure 6 shows the results of a bifurcation analysis for a domain with aspect ratio $a = 1$ and angle $\varphi = 67.5°$. The bottom right panel is the bifurcation diagram in the X-plane, with the values of X for which examples are shown indicated by the lettered points. The remainder of the panels show the advecting vortex systems and their separatrices for each of these example values of X. Note that the diagonals of
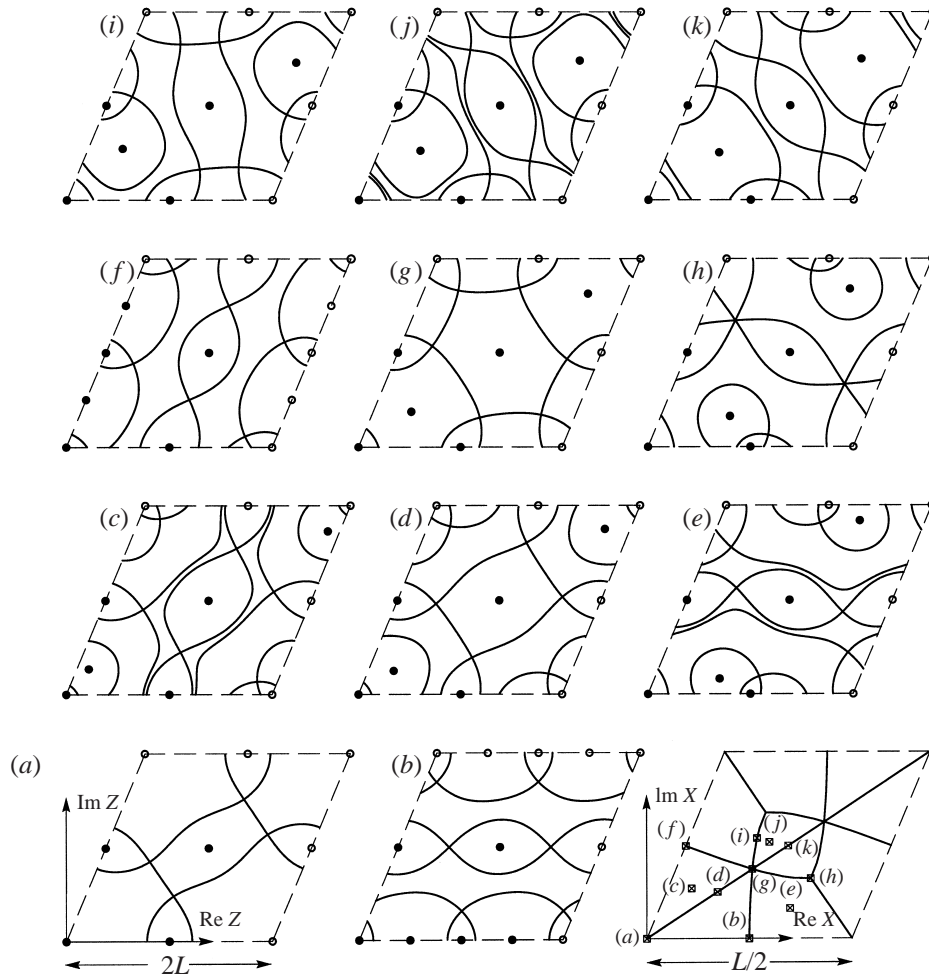
FIGURE 6. Bifurcation diagram in X-space (lower right) and representative streamline patterns in the field of the stationary phase-space vortices (panels $(a\text{–}k)$) for $\gamma = 0$ and a domain with aspect ratio $a = |\omega_2|/|\omega_1| = 1$ and angle $\varphi = 67.5°$ between the half-periods ω_1 and ω_2.

the parallelogram are axes of symmetry for the bifurcation diagram, and thus, based on our argument at the end of §4.2, it is necessary to examine only one-fourth of the possible X values. From figure 6 we see that merely changing the shape of the domain has increased the number of regimes in the bifurcation diagram to ten, with the two centre regimes yielding qualitatively new streamline patterns. For example, panels (j) and (k) each have two regimes of motion in which the trajectory of a particle at Z increases without bound in a direction that is not parallel to either period of the parallelogram. The streamline patterns in figure 5 show that this type of motion cannot occur in a square domain. Panel (j), for which $X = L(0.6 + i0.48)/2$, has been reproduced in the top left panel of figure 7 with corresponding real-space motions of the vortices shown in panels labelled I–IX. The unbounded regimes of interest, which correspond to wandering motions in real space, are labelled VIII and IX. Regimes I–IV correspond to paired motions, regimes V and VI to coupled motions, and regime VII to collective motion. It is interesting to compare the vortex trajectories in figure 7 with those in figure 4.
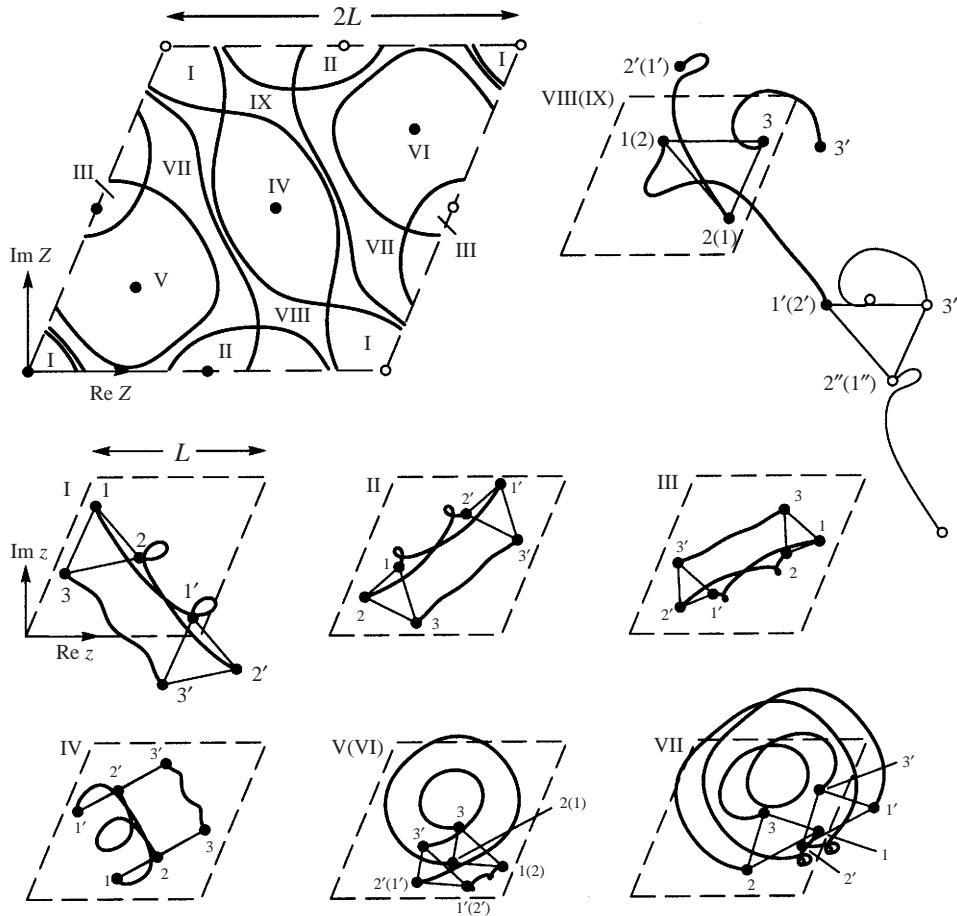
FIGURE 7. Streamline pattern (top left) corresponding to the X-value at point (j) in the bifurcation diagram of figure 6 and representative vortex trajectories (panels I–IX) from each of the nine regimes.

Figure 8 shows the results of a bifurcation analysis for a rectangular domain with aspect ratio $a = 1.25$. The bottom right panel is the bifurcation diagram in the X-plane, with the values of X at which examples are shown indicated by the lettered points. The remainder of the panels show the advecting vortex systems and their separatrices for each of these example values of X. The most interesting qualitative difference between this and our previous results is the possibility of having wandering motions with $X = 0$, which is not possible for $a = 1$ regardless of the angle φ.

We have explored more fully how changing the domain shape affects the results of the bifurcation analysis, including different choices of aspect ratio a and angle φ. We have observed qualitative changes in the bifurcation diagram at, for example, aspect ratios above $a = \sqrt{2}$ for a rectangular domain. However, we feel the results presented here provide an adequate description of the type of behaviour possible in this system. It is interesting to note that simply changing the domain shape introduces new qualitative behaviour in the system. This may have implications for numerical simulations of two-dimensional turbulence, which are typically conducted only in square periodic domains.
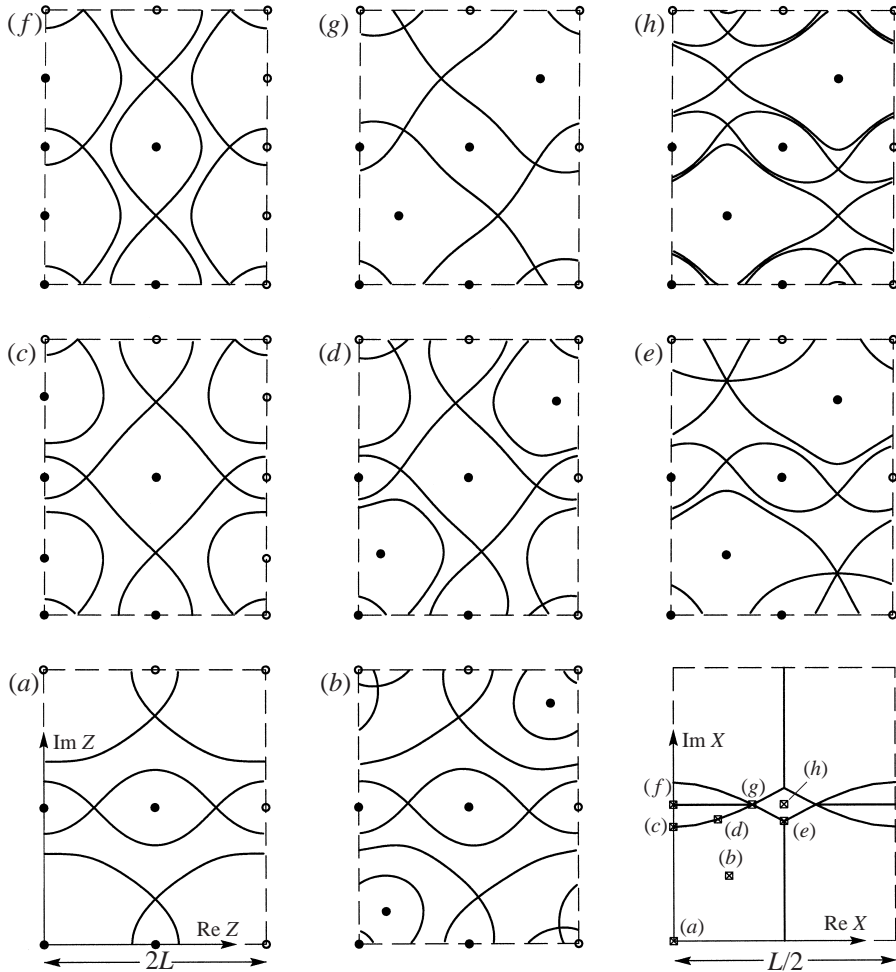
FIGURE 8. Bifurcation diagram in X-space (lower right) and representative streamline patterns in the field of the stationary phase-space vortices (panels (a–h)) for $\gamma = 0$ and a rectangular domain with aspect ratio $a = 1.25$.

5. Results for non-zero rational γ

In this Section we restrict our investigation to non-zero rational values of γ, with $\gamma = p/q$ in lowest terms. From the analysis of §3, the equation of motion for the advected particle at Z can be written as in (3.19). This general analysis shows that the advection problem can be represented in a parallelogram with half-periods $2q\omega_1$ and $2q\omega_2$. However, for certain cases the advection problem is periodic in a smaller parallelogram.

Without loss of generality consider a shift of the base vortices in which base vortex 1 is shifted by $2a\omega_1 + 2b\omega_2$, base vortex 2 by $2c\omega_1 + 2d\omega_2$, and base vortex 3 is not shifted at all. This changes Z by $2(a - c)\omega_1 + 2(b - d)\omega_2$. In order to ensure that we are considering an equivalent problem, we require that X is not changed, i.e. a and c must satisfy $(\gamma + \frac{1}{2})a = (\gamma - \frac{1}{2})c$, and b and d must satisfy $(\gamma + \frac{1}{2})b = (\gamma - \frac{1}{2})d$. With $\gamma = p/q$ this means, for example, that $2p(c - a) = q(c + a)$. We are only interested in $q > 2$. Consider first the case where q is odd. Since p and q are relatively prime, this

relation tells us that $c + a$ must be a multiple of p and $c - a$ must be a multiple of q, i.e. there must exist an integer h such that $c - a = hq$ and $c + a = 2hp$. Solving for a and c we have $2a = h(2p - q)$ and $2c = h(2p + q)$. Since q is odd, it follows from these equations that h must be even. Similarly, we must have $2b = k(2p - q)$ and $2d = k(2p + q)$ with k even. The smallest shift in Z that leads to an equivalent problem thus occurs for $h = k = 2$, from which we conclude that the phase space will be periodic with half-periods $2q\omega_1$ and $2q\omega_2$ and we should not expect smaller periods. We have already seen that there are $6q^2 + 8p^2$ stationary vortices in the basic phase-space parallelogram for this case.

For even q the situation is different. We set $q = 2u$ and note that p must now be odd. The equation $2p(c - a) = q(c + a)$, for example, becomes $p(c - a) = u(c + a)$, where u and p are relatively prime. There then exists an h such that $c - a = hu$ and $c + a = hp$, from which $2a = h(p - q)$ and $2c = h(p + q)$. Now, if u is odd, $p + u$ is even, and $h = 1$ gives the smallest value of $c - a$, namely $q/2$. On the other hand, if u is even, h must also be even, and the smallest value of $c - a$ occurs for $h = 2$ and is q. The results are similar for the integers b and d. Thus, if q is divisible by 4 the phase space is periodic with half-periods $q\omega_1$ and $q\omega_2$ and there are $(6q^2 + 8p^2)/4$ stationary vortices in the basic phase-space parallelogram. If q is even but not divisible by 4, the phase space is periodic with half-periods $(q/2)\omega_1$ and $(q/2)\omega_2$ and there are $(6q^2 + 8p^2)/16$ stationary vortices in the basic phase-space parallelogram.

5.1. *The case $\gamma = \frac{1}{6}$*

Among the simplest rational values of γ to consider are $p/q = \frac{1}{3}$ and $\frac{1}{4}$ corresponding to the vortex strength ratios $\Gamma_1 : \Gamma_2 : \Gamma_3 = 5 : 1 : (-6)$ and $3 : 1 : (-4)$, respectively. In the first case q is odd and the advection of a particle at Z occurs in the field of 62 stationary vortices in a parallelogram with half-periods $6\omega_1$ and $6\omega_2$. For $q = 4$ the advection is by 26 stationary vortices in a parallelogram with half-periods $4\omega_1$ and $4\omega_2$. However, for $\gamma = \frac{1}{6}$, which corresponds to the vortex strength ratios $\Gamma_1 : \Gamma_2 : \Gamma_3 = 2 : 1 : (-3)$, q is even but not divisible by 4, so that the advection is by 14 vortices in a parallelogram with half-periods $3\omega_1$ and $3\omega_2$. Thus $\frac{1}{6}$ is the simplest non-zero rational value for γ because it yields the smallest periodic domain in phase space with the smallest number of stationary vortices.

Figure 9 shows the results of a bifurcation analysis for $\gamma = \frac{1}{6}$ in a square domain. The bottom right panel is the bifurcation diagram in the X-plane and the other three panels are the advecting vortex systems and their separatrices for the example values of X indicated by the labels (*a–c*). The streamline pattern corresponding to the value of X at point (*d*) is shown in figure 10. The bifurcation diagram in X for this case is already much more complex than the corresponding diagram for $\gamma = 0$ in figure 5. This is because in general there are the same number of zeros (stagnation points) in the Z-plane as there are poles (stationary vortices), and the bifurcation diagram indicates the values of X for which the stagnation points are connected by separatrices.† The bifurcation diagram for this case analyses how the 14 stagnation points 'join up', while the analysis for $\gamma = 0$ involves only four stagnation points. In fact, the analysis for $\gamma = 0$ is simplified further by the symmetry imposed by taking $\Gamma_1 = \Gamma_2$.

---

† The theory of elliptic functions states that the sum of the order of the zeros must equal the sum of the order of the poles in the parallelogram (Whittaker & Watson 1927, §20.14). For example, in panel (*h*) of figure 5, there are six vortices but only two stagnation points. The vortices are first-order poles, and in this case the stagnation points are third-order zeros (each of them is formed by the coalescence of three first-order zeros) so that the sum of the order of either poles or zeros, with multiplicities taken into account, is six.
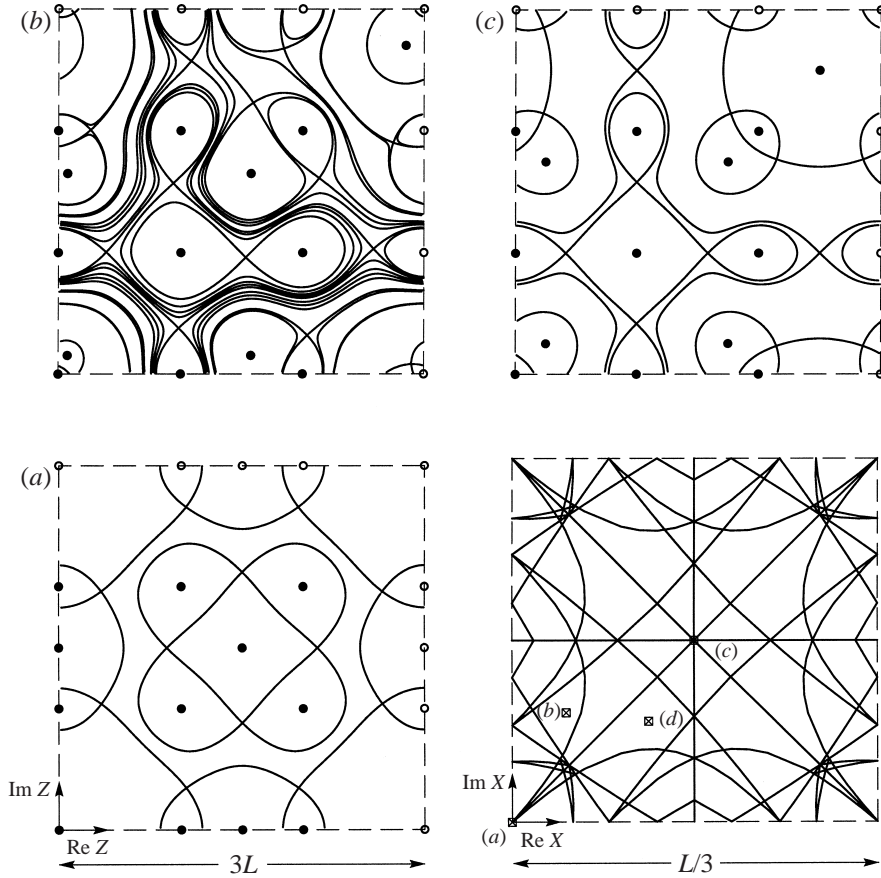
FIGURE 9. Bifurcation diagram in X-space (lower right) and representative streamline patterns in the field of the stationary phase-space vortices (panels (a–c)) for $\Gamma_1 : \Gamma_2 : \Gamma_3 = 2 : 1 : (-3)$, or $\gamma = \frac{1}{6}$, and a square domain. Streamline pattern corresponding to (d) is in figure 10.

Of the four X values indicated in the bifurcation diagram of figure 9, those labelled (a) and (c) are on bifurcation curves and thus exhibit a degeneracy or symmetry with two or more stagnation points in the phase-space streamline pattern connected by separatrices. In contrast, the streamline patterns shown in panel (b) of figure 9 and in figure 10 are non-degenerate. We consider in some detail the pattern shown in figure 10 with $X = L(0.375 + i0.2775)/3$. There are 27 regimes of motion, but we only consider the motion in seven of the regimes. Just by observing the structure of the streamline pattern we can conclude that regime I corresponds to paired motion, regimes IV and VI to coupled motions, regimes II, V, and VII to collective motions, and regime III to wandering motion.

As pointed out in AS, it is important to note that the approximate dipole structures seen in figure 10, such as the one containing regimes I and IV, are essential features of the streamline pattern and are the main new feature arising for $\gamma \neq 0$. For non-degenerate streamline patterns the stagnation points display this 'disconnected' topology, i.e. the saddle points in the phase-space diagram are homoclinic rather than heteroclinic. This gives rise to regimes of motion that reside in very thin strips of phase space, such as regime II in figure 10, yet are clearly identifiable in the real-space dynamics of the vortices. In fact, some of the regimes in figure 10 are so thin that they are unresolved at the resolution shown! Yet despite the thinness of some of
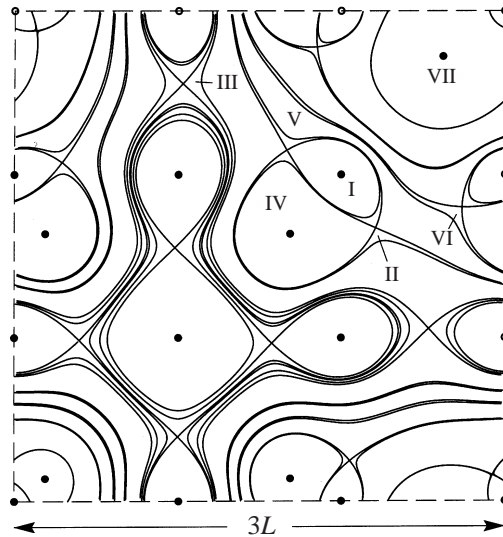
FIGURE 10. Phase space in a square domain for $\gamma = \frac{1}{6}$ and a non-degenerate value of $X = L(0.375 + i0.2775)/3$ (point (*d*) on the bifurcation diagram of figure 9). The sides of the domain have length $3L$ and there are 14 stationary vortices (solid dots). The regimes we investigate are labelled I–VII.

these collective- and wandering-motion regimes, there are sufficiently many of them to account for a significant area of the phase space.

In figure 11 we show representative real-space trajectories corresponding to the seven labelled regimes of figure 10. The paired motion in panel I and the coupled motions in panels IV and VI are not much different from what we have already observed in the case $\gamma = 0$. However, the collective motions in panels II, V, and VII and the wandering motion in panel III are extremely complex with the vortices moving through a sequence of complicated turns, some of which are quite sharp. We stress that the relative vortex motion for all cases shown in figure 11 is periodic, and that each of these trajectories has an infinite number of periodic images tiling the complex plane. The re-emergence of the vortex configuration in a wandering motion such as panel III requires consideration of periodic images.

As pointed out in AS for the periodic strip, an interesting corollary of all these developments is that there are no stable steady configurations of the three vortices in real space. Steady configurations correspond to stagnation points of the advecting flow in phase space away from the vortices, and since these are all saddle points, the corresponding configurations must be unstable. It is clear that these unstable states and the separatrix motions connecting them provide a 'skeleton' from which the full dynamics can be understood.

5.2. *The case* $\gamma = \frac{1}{5}$

As an example of how complicated this integrable problem becomes, consider the case $\gamma = \frac{1}{5}$ in a square with $X = L(0.3 + i0.2)/5$. The corresponding advecting vortex system and its separatrices are shown in figure 12. Here $q = 5$ is odd, so that the advection problem takes place in a square of side $10L$ and there are $8p^2 + 6q^2 = 158$ stationary vortices. It is difficult to tell if this choice of X corresponds to a degenerate or non-degenerate case, as some of the regimes in phase space are so thin that the resolution of our numerical scheme for drawing separatrices fails to identify them. In either case we have an extremely complex phase-space streamline pattern with
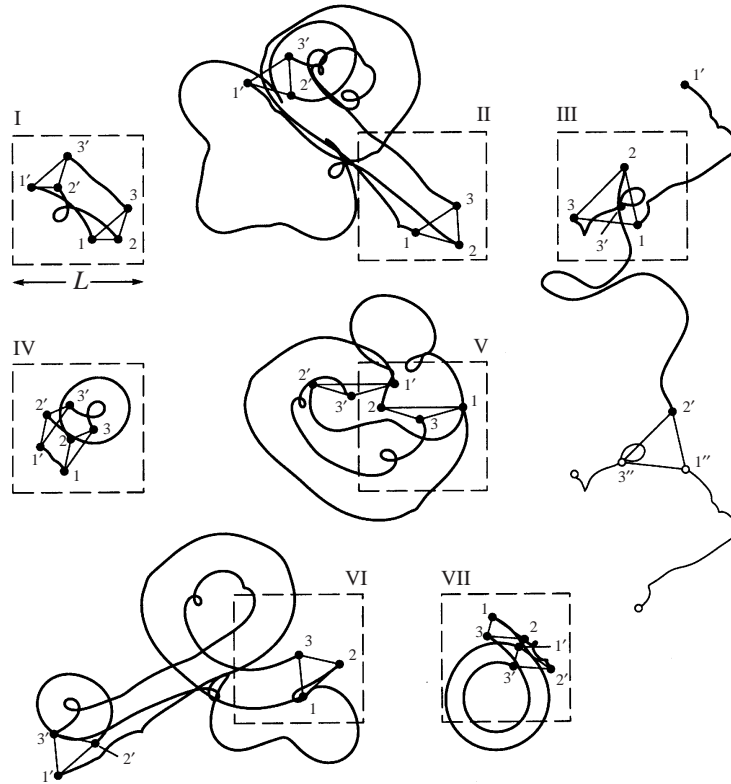
FIGURE 11. Real-space trajectories of the three vortices with $\gamma = \frac{1}{6}$ and $X = L(0.375 + i0.2775)/3$ corresponding to the regimes labelled I–VII in figure 10.

over 275 different regimes of motion! We investigate the motions in only the seven regimes labelled I–VII, and show the corresponding real-space trajectories in figure 13. Panel II displays coupled motion (vortices 1 and 3 orbit one another) and is similar to other coupled motions we have observed. Panels III and IV are examples of collective motion corresponding to the particle at Z in phase space orbiting only a few of the stationary vortices. Panels I, V, and VI also display collective motions, but the corresponding particles at Z in phase space now orbit several of the stationary vortices. In fact, regime VI in figure 12 contains the longest possible path in this phase space. If we were to trace out the path of an advected particle at Z in regime VI of figure 12, it would look very similar to the path traced out by vortex 2 in panel VI of figure 13. Panel VII shows a sample trajectory for wandering motion. We stress that the motion in panels VI and VII takes place over an area that is many times the area of the basic periodic $L \times L$ square (shown by the dashed line in figure 13).

6. The case of irrational γ

In general γ will, of course, be irrational. As was the case for the periodic strip discussed in AS, the procedure given in §3 for rational γ does not immediately generalize and does not converge in a simple way if one considers a sequence of rational approximants, p_i/q_i, approaching the irrational γ ever more closely. For each of these approximants the procedure of §3 may be applied. The problem is that the
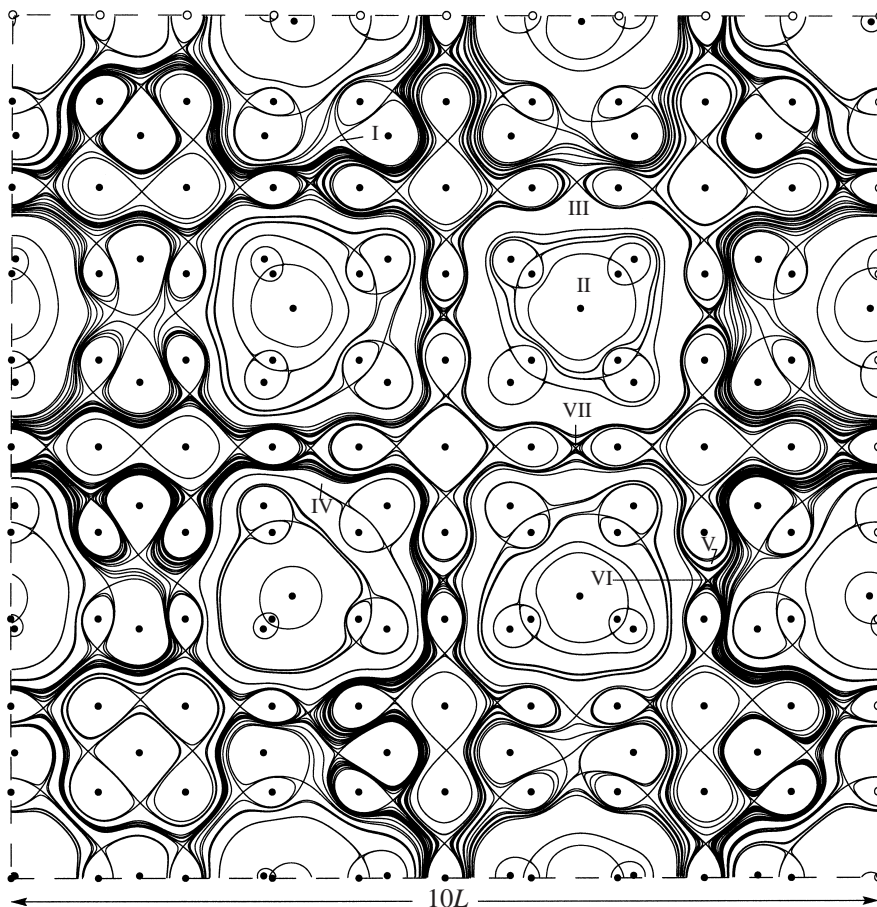
FIGURE 12. Phase-space in a square domain for $\Gamma_1 : \Gamma_2 : \Gamma_3 = 7 : 3 : (-10)$, or $\gamma = \frac{1}{5}$, and $X = L/5\,(0.3 + i0.2)$. The sides of the domain have length $10L$ and there are now 158 stationary vortices (solid dots). The regimes we investigate are labelled I–VII.

denominators q_i may fluctuate considerably so that one is led to consider successive parallelograms and vortex patterns that vary greatly in size.

Instead, for irrational γ return to the equation of motion for Z given in (3.5). By the definition of the Weierstrass ζ-function (2.1) this equation can be written as

$$\frac{\mathrm{d}\bar{Z}}{\mathrm{d}t} = -\frac{\Gamma_3}{2\pi\mathrm{i}} \left\{ \frac{1}{Z} + {\sum_{(m,n)}}' \left[\frac{1}{Z - \Omega_{mn}} + \frac{1}{\Omega_{mn}} + \frac{Z}{\Omega_{mn}{}^2} \right] \right.$$

$$- \frac{1}{\left(\frac{1}{2}+\gamma\right)Z - X} - {\sum_{(m,n)}}' \left[\frac{1}{\left(\frac{1}{2}+\gamma\right)Z - X - \Omega_{mn}} + \frac{1}{\Omega_{mn}} + \frac{\left(\frac{1}{2}+\gamma\right)Z - X}{\Omega_{mn}{}^2} \right]$$

$$\left. - \frac{1}{\left(\frac{1}{2}-\gamma\right)Z + X} - {\sum_{(m,n)}}' \left[\frac{1}{\left(\frac{1}{2}-\gamma\right)Z + X - \Omega_{mn}} + \frac{1}{\Omega_{mn}} + \frac{\left(\frac{1}{2}-\gamma\right)Z + X}{\Omega_{mn}{}^2} \right] \right\},$$

$$(6.1a)$$

where the summations are over all pairs of integers $(m,n) \neq (0,0)$. Combining the
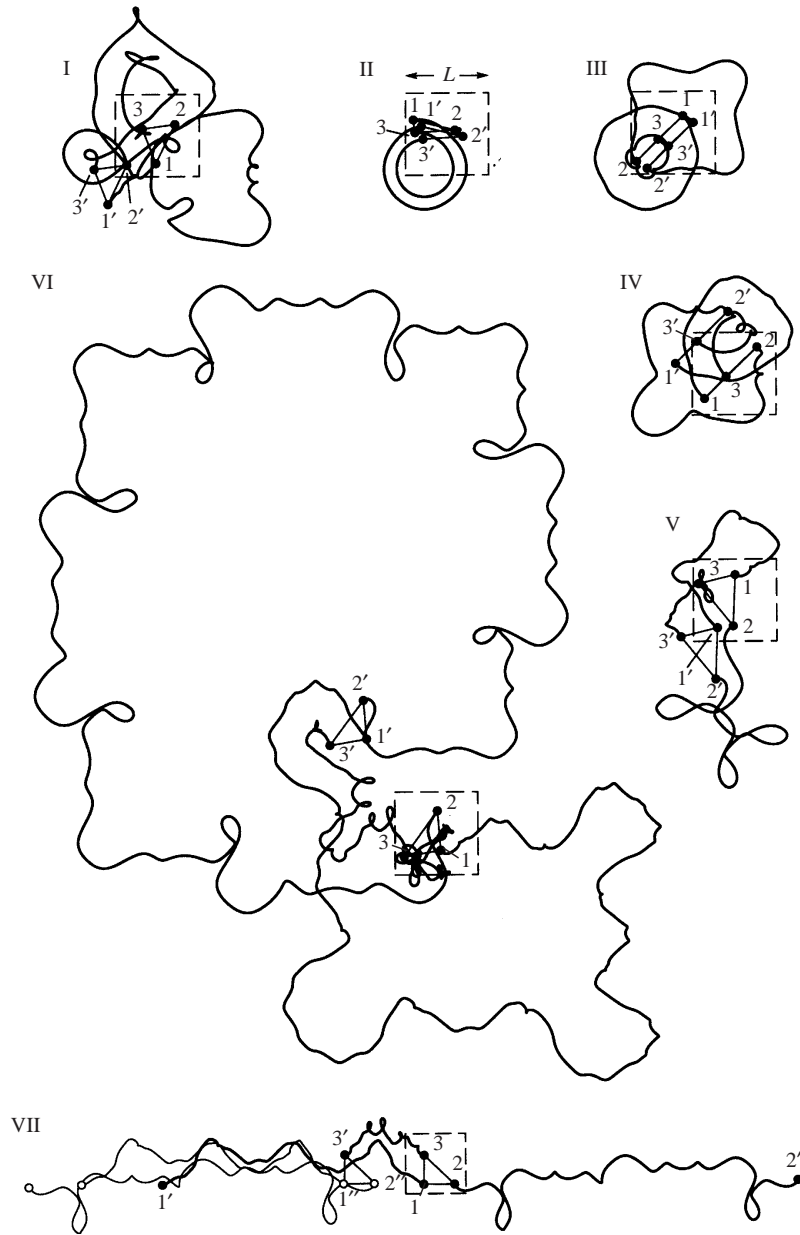
FIGURE 13. Real-space trajectories of the three vortices with $\gamma = \frac{1}{5}$, and $X = L(0.3 + \mathrm{i}0.2)/5$ corresponding to the regimes labelled I–VII in figure 12. Note smaller scale of motion in regime VII.

summation terms gives

$$
\frac{\mathrm{d}\bar{Z}}{\mathrm{d}t} = -\frac{\Gamma_3}{2\pi\mathrm{i}} \left\{ \frac{1}{Z} - \frac{1}{\left(\frac{1}{2} + \gamma\right) Z - X} - \frac{1}{\left(\frac{1}{2} - \gamma\right) Z - X} \right.
$$

$$
\left. - \sideset{}{'}\sum_{(m,n)} \left[\frac{1}{Z - \Omega_{mn}} - \frac{1}{\left(\frac{1}{2} + \gamma\right) Z - X - \Omega_{mn}} - \frac{1}{\left(\frac{1}{2} - \gamma\right) Z + X - \Omega_{mn}} - \frac{1}{\Omega_{mn}} \right] \right\}.
$$

$$(6.1b)$$

The goal is to interpret (6.1*b*) as the equation of motion for a passive particle in the field of three infinite families of vortices on the unbounded plane, which requires that each of the terms in the summand of (6.1*b*) be treated separately. Since sums over each of the individual terms in the summand are conditionally convergent some ordering of the summation must be imposed. We denote such an ordered sum by $\sum_{m,n}$. Equation (6.1*b*) can thus be written as

$$\frac{\mathrm{d}\bar{Z}}{\mathrm{d}t} = -\frac{\Gamma_3}{2\pi\mathrm{i}} \sum_{m,n} \left\{ \frac{1}{Z - \Omega_{mn}} - \frac{1}{\frac{1}{2} + \gamma} \left(\frac{1}{Z - (\Omega_{mn} + X)/(\frac{1}{2} + \gamma)} \right) \right.$$
$$\left. - \frac{1}{\frac{1}{2} - \gamma} \left(\frac{1}{Z - (\Omega_{mn} - X)/(\frac{1}{2} - \gamma)} \right) \right\} \quad (6.2)$$

in a frame translating with conjugate velocity $-\Gamma_3/2\pi\mathrm{i} \sum_{m,n}' 1/\Omega_{mn}$. The value of this translation velocity depends on the ordering of the sum. Physically, we expect the infinite problem governed by (6.1*b*) to be consistent with the previous results for rational γ, i.e. we expect this infinite system of vortices to be stationary, which requires that the sums be ordered so that the translation velocity is zero. This result shows that for any γ, including irrational values, there is a mapping of the real-space problem onto an advection problem for a passive particle in the field of a system of stationary vortices that belong to one of three infinite families. Whereas for rational γ these three families form a pattern that is periodic in a domain which is a multiple of the original domain, for irrational γ no such parallelogram exists. The incommensurability of the lattice spacings means that an infinite system is required.

As illustrated in the streamline patterns of figures 10 and 12, the saddle points in phase space in general do not 'join up'. Thus for the case of irrational γ it appears that, except for a special set of X-values, no two stagnation points in the advection problem will be joined by a separatrix, leading to an infinity of regimes of motion. There will still exist the four types of regimes corresponding to paired, coupled, collective and wandering motions. However, the regimes corresponding to wandering motions will necessarily extend to infinity, leading to real-space motions that are not periodic, even with the consideration of periodic images.

7. Concluding remarks

Regardless of the value of the vortex strengths, the problem of three point vortices in a doubly periodic domain can be mapped to the problem of advection of a passive particle by a system of stationary vortices. If the ratio of the vortex strengths is rational then the relative motion of the vortices in real space is periodic in time; if this ratio is irrational then the relative vortex motion can be aperiodic. In both cases there exist regimes of motion in which the vortex trajectories are more complicated than expected from an integrable system.

McWilliams (1990; see, in particular, his figure 2) has attempted to trace individual, concentrated vortices in large-scale numerical simulations of two-dimensional turbulence. He finds vortex trajectories that share qualitative features with those of the three-vortex problem. An individual vortex in the simulations negotiates sharp turns and long, relatively uneventful flights of several periodic box lengths. Finite-area vortices also may merge with other vortices in the field, and may undergo substantial straining, so complete correspondence with point vortex trajectories is not to be expected. Nevertheless, our solutions of the three-vortex problem provide support for

the conclusion that the complexity of individual vortex trajectories observed in two-dimensional turbulence is not necessarily associated with the turbulent field. Vortex trajectories of comparable complexity are readily found in the integrable three-vortex problem in a periodic square. This observation, along with a study of the advection properties of three-vortex motion in a periodic square, have suggested to us that the problem of three vortices in a periodic parallelogram, suitably averaged over vortex circulations, and over initial conditions, may provide a useful and tractable model of two-dimensional turbulence. We are currently pursuing this idea.

REFERENCES

ACZÉL, J. 1969 *On Applications and Theory of Functional Equations*. Academic.

AREF, H. 1989 Three-vortex motion with zero total circulation: Addendum. *Z. Angew. Math. Phys.* **40**, 495–500.

AREF, H. & STREMLER, M. A. 1996 On the motion of three point vortices in a periodic strip. *J. Fluid Mech.* **314**, 1–25 (referred to herein as AS).

BENZI, R. & LEGRAS, B. 1987 Wave–vortex dynamics. *J. Phys.* A **20**, 5125–5144.

CAMPBELL, L. J., DORIA, M. M. & KADTKE, J. B. 1989 Energy of infinite vortex lattices. *Phys. Rev.* A **39**, 5436–5439.

MCWILLIAMS, J. C. 1990 The vortices of two-dimensional turbulence. *J. Fluid Mech.* **219**, 361–385.

O'NEIL, K. A. 1989 On the Hamiltonian dynamics of vortex lattices. *J. Math. Phys.* **30**, 1373–1379.

ROTT, N. 1989 Three-vortex motion with zero total circulation. *Z. Angew. Math. Phys.* **40**, 473–494.

STREMLER, M. A. & AREF, H. 1996 Motion of three point vortices in a periodic domain. *Bull. Am. Phys. Soc.* **41**, 1757.

TKACHENKO, V. K. 1966 On vortex lattices. *Sov. Phys. JETP* **22**, 1282–1286.

WEISS, J. B. & MCWILLIAMS, J. C. 1991 Nonergodicity of point vortices. *Phys. Fluids* A **3**, 835–844.

WHITTAKER, E. T. & WATSON, G. N. 1927 *A Course of Modern Analysis*. Cambridge University Press.